

THE $u'g'r'i'z'$ STANDARD-STAR SYSTEM

J. ALLYN SMITH,^{1,2,3} DOUGLAS L. TUCKER,⁴ STEPHEN KENT,⁴ MICHAEL W. RICHMOND,⁵ MASATAKA FUKUGITA,^{6,7}
TAKASHI ICHIKAWA,⁸ SHIN-ICHI ICHIKAWA,⁹ ANDERS M. JORGENSEN,¹⁰ ALAN UOMOTO,¹¹ JAMES E. GUNN,¹²
MASARU HAMABE,¹³ MASARU WATANABE,¹⁴ ALIN TOLEA,¹¹ ARNE HENDEN,¹⁵ JAMES ANNIS,⁴
JEFFREY R. PIER,¹⁵ TIMOTHY A. MCKAY,¹ JON BRINKMANN,¹⁶ BING CHEN,¹¹ JON HOLTZMAN,¹⁷
KAZUHIRO SHIMASAKU,¹⁸ AND DONALD G. YORK¹⁹

Received 2001 October 23; accepted 2001 December 20

ABSTRACT

We present the 158 standard stars that define the $u'g'r'i'z'$ photometric system. These stars form the basis for the photometric calibration of the Sloan Digital Sky Survey. The defining instrument system and filters, the observing process, the reduction techniques, and the software used to create the stellar network are all described. We briefly discuss the history of the star selection process, the derivation of a set of transformation equations for the $UBVR_C I_C$ system, and plans for future work.

Key words: catalogs — standards — stars: fundamental parameters

1. INTRODUCTION

We present the newly established standard-star network for the $u'g'r'i'z'$ filter system (see Fukugita et al. 1996). This standard-star network was developed at the US Naval Observatory (USNO), Flagstaff Station. These stars form the basis for the photometric calibration of the Sloan Digital Sky Survey (SDSS). The SDSS uses a 2.5 m telescope at Apache Point Observatory (APO) to produce a five-band,

photometrically calibrated digital imaging survey of π steradians ($10,000 \text{ deg}^2$) of the northern Galactic cap (Gunn et al. 1998; York et al. 2000) as one of its major data products.

It is not our purpose here to describe in detail the full end-to-end process of calibrating the SDSS photometric data. That is the topic of a future paper. Here we merely wish to present a self-contained description of the standard-star network upon which the SDSS photometry is based. We do note, however, that one of the targets of the SDSS is to achieve a level of photometric uniformity and accuracy such that the systemwide rms errors in the final SDSS photometric catalog will be less than 0.02 mag in r' , 0.02 mag in $r'-i'$ and $g'-r'$, and 0.03 mag in $u'-g'$ and $i'-z'$, for objects bluer than an M0 dwarf. To meet this target, internal goals were set for the accuracy of the primary standard star system: the uncertainty in the mean calibrated magnitudes for any given primary standard star should be $\leq 1.5\%$ at u' , $\leq 1\%$ in g' , r' , and i' , and $\leq 1.5\%$ at z' . As we will show later in this paper, we more than meet these goals for all but a handful of stars.

In addition, we must mention that because of small but significant differences between the USNO and 2.5 m filters, the final 2.5 m SDSS published photometry will likely differ systematically from the $u'g'r'i'z'$ system at the few-percent level for $g'r'i'$, and slightly worse for u' and z' (see Stoughton et al. 2002). When transformation equations between the $u'g'r'i'z'$ system and the 2.5 m SDSS photometry have been robustly determined, they will be promptly made available to the astronomical community. (Note that the intended accuracy of these transformation equations is included within the aforementioned error budget for the photometric calibrations of the final SDSS imaging catalog.)

The nomenclature used in this system differs slightly from the traditional photometric literature. This was done to avoid confusion with existing SDSS papers and nomenclature. In the traditional sense, Vega (α Lyr) is the ultimate “fundamental” standard. However, in this paper we refer to three subdwarf stars that were used to set the initial system zero point as “fundamental,” with the other 155 stars of the system being referred to as “primary” stars. The term “secondary” is used within the SDSS nomenclature to refer to the photometric system transfer patches—pieces of the sky that are observed by a 0.5 m telescope that are used to

¹ Department of Physics, University of Michigan, 500 East University, Ann Arbor, MI 48109-1120.

² Visiting Astronomer, US Naval Observatory.

³ Current address: Department of Physics and Astronomy, University of Wyoming, P.O. Box 3905, Laramie, WY 82071.

⁴ Fermi National Accelerator Laboratory, P.O. Box 500, Batavia, IL 60510.

⁵ Department of Physics, Rochester Institute of Technology, 85 Lomb Memorial Drive, Rochester, NY 14623-5603.

⁶ Institute for Cosmic Ray Research, University of Tokyo, 3-2-1 Midori, Tanashi, Tokyo 188-8502, Japan.

⁷ Institute for Advanced Study, Einstein Drive, Princeton, NJ 08540.

⁸ Astronomical Institute, Tohoku University, Aramaki, Aoba, Sendai 980-8578, Japan.

⁹ National Astronomical Observatory, 2-21-1 Osawa, Mitaka, Tokyo 181-8588, Japan.

¹⁰ Los Alamos National Laboratory, Mail Stop D448, P.O. Box 1663, Los Alamos, NM 87545.

¹¹ Department of Physics and Astronomy, Johns Hopkins University, 3400 North Charles Street, Baltimore, MD 21218.

¹² Princeton University Observatory, Peyton Hall, Princeton, NJ 08544-1001.

¹³ Department of Mathematical and Physical Sciences, Japan Women’s University, 2-8-1 Mejirodai, Bunkyo, Tokyo 112-8681, Japan.

¹⁴ Institute of Space and Astronautical Science, 3-1-1 Yoshinodai, Sagamihara, Kanagawa 229-8510, Japan.

¹⁵ US Naval Observatory, Flagstaff Station, P.O. Box 1149, Flagstaff, AZ 86002.

¹⁶ Apache Point Observatory, P.O. Box 59, Sunspot, NM 88349.

¹⁷ Department of Astronomy, MSC 4500, New Mexico State University, P.O. Box 30001, Las Cruces, NM 88003.

¹⁸ Department of Astronomy and Research Center for the Early Universe, University of Tokyo, 7-3-1 Hongo, Bunkyo, Tokyo 113-0033, Japan.

¹⁹ Enrico Fermi Institute and Department of Astronomy and Astrophysics, University of Chicago, 5640 South Ellis Avenue, Chicago, IL 60637.

transfer the photometric solution to the main survey imaging telescope.

In the following sections, we present details of the standard-star development program. We describe the instrumentation and filter system in § 2 and selection of the initial set of stars in § 3, and we give a brief overview of the reduction software that was used to develop the network in § 4. Final results for the initial set of $u'g'r'i'z'$ primary standard stars are presented in § 5, and we discuss future extensions to this system in § 6.

2. OBSERVATIONS AND INSTRUMENTATION

The observations were obtained using the 1.0 m Ritchey Chrétien telescope at the USNO Flagstaff Station during the bright period of each lunation from 1998 March through 2000 January, inclusive. Since the program stars were fairly bright, the Moon did not unduly hamper the observations; however, we did maintain a minimum 30° radius of avoidance near the Moon that, for the most part, allowed us to use the dome to shield the telescope from direct moonlight. This observing restriction had a slight impact on the choice of stars observed each night. The few “faint” stars (fainter than about $r' = 13.2$) on the list were observed when the Moon was below or within 1 hr of the opposite horizon from the star, so the dome could be used to block the Moon completely.

All of the observations were direct exposures with a thinned, UV/antireflection-coated Tektronix TK1024 CCD operating at a gain of $7.43 \pm 0.41 e^- \text{ ADU}^{-1}$ with a read noise of $6.0 e^-$. This CCD is similar to the CCDs used in the

main SDSS survey camera and the CCD used by the 0.5 m photometric monitoring telescope at APO. The camera scale of 0.68 pixel^{-1} produced a field of view of $11.54'$.

Testing of the chip revealed a linear response up to 15,200 ADU and a second, well-behaved and correctable linear-response region up to 27,500 ADU (see Fig. 1). This change in the CCD response function, and sense of the change, is due to the clocking scheme that was employed in the TK1024 read electronics. The integration and the lowering of the transfer gate occurred simultaneously. The net result is that, since the summing well has more charge for brighter objects, the charge begins to “spill over” the gate potential faster for these objects, resulting in an effectively longer integration time (and a seemingly higher gain) than for the faint objects.

Exposure lengths were tailored to maximize the number of potential standard stars in each field with good photon counts in all five filters while not exceeding the first linear portion of the response curve for the primary star of interest. Tailoring the exposure lengths allowed us to develop multiple standards in several fields. Use of the linearity response curve allowed correction of the brighter stars when good atmospheric seeing caused counts greater than 15,200 ADU pixel^{-1} , while allowing us to maximize observing efficiency in some of the more populated fields. The drawback of targeting multiple stars per field was a decrease in the signal-to-noise ratio for the extreme red or blue stars within the same field for which the exposures were not optimized.

The five filters of the $u'g'r'i'z'$ system have effective wavelengths of 3540, 4750, 6222, 7632, and 9049 Å, respectively, at 1.2 air masses.²⁰ They cover the entire wavelength range of the combined atmosphere-plus-CCD response, and their construction is described by Fukugita et al. (1996). Also shown in that paper (their Fig. 1) are the designed response curves for the filters multiplied by the quantum-efficiency curve of a thinned, UV/antireflection-coated Tektronix TK1024 CCD similar to the detector that was used in the development of this standard system. The $u'g'r'i'z'$ filters have sharp cutoffs by design. The passbands were selected to exclude the strongest night-sky lines, for example, O I ($\lambda 5577$) and Hg I ($\lambda 5461$). The bulk of the u' -band response is blueward of the Balmer discontinuity, which, when combined with the g' filter, yields high sensitivity to the magnitude of the Balmer jump, but at a cost of lower throughput for the narrower u' filter (compared with Johnson U). In Figure 2, we show the filter responses multiplied by the sensitivity data for a CCD similar to that used to set up the $u'g'r'i'z'$ system. These curves represent the expected total quantum efficiencies of the filter transmissions, the quantum efficiency of the CCD surface, and the reflections from two aluminum mirror surfaces. The two sets of response curves shown are for the case without atmospheric extinction (*upper curves*) and as modified for typical extinctions at 1.2 air masses (*lower curves*). Figure 3 compares the (normalized) $UBVR_C I_C$ filter curves with those of the $u'g'r'i'z'$ system.

The filter transmission data as measured by the Japan Participation Group within the SDSS, the filter manufacturing specifications and the CCD-plus-filter response curves

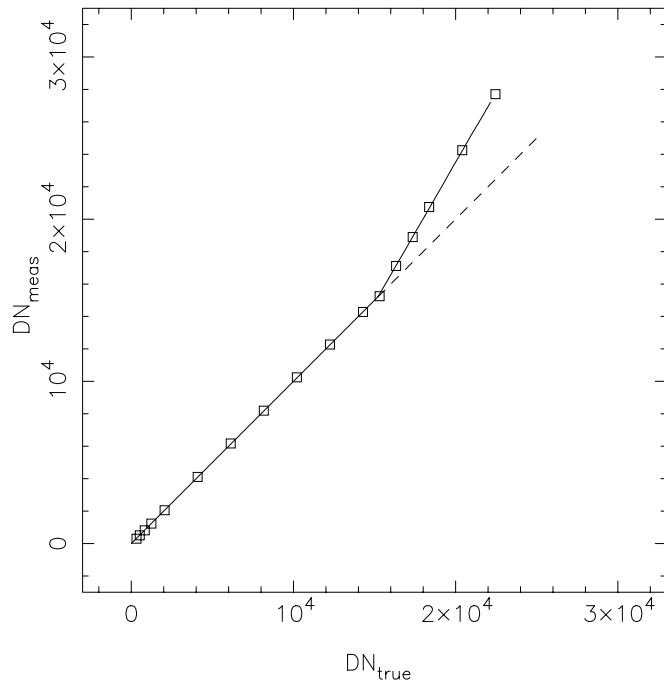


FIG. 1.—Linearity curve for the TK1024 CCD used on the USNO 1.0 m telescope for this program (*solid line*). DN_{meas} is the raw, bias-subtracted value of the signal; DN_{true} is the value that would have been measured if the CCD were completely linear. Note the “knee” at $DN \approx 15,200$ ADU. The dashed line acts as a reference for what a fully linear relation would look like.

²⁰ Note that the g' filter has been determined to have an effective wavelength 20 Å bluer than that originally quoted by Fukugita et al. (1996).

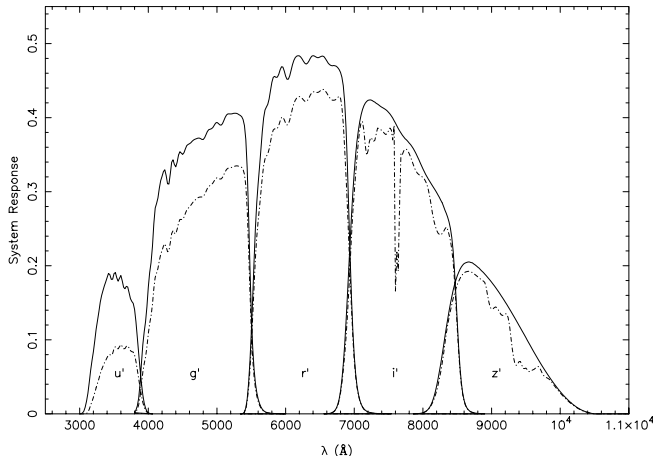


FIG. 2.—The $u'g'r'i'z'$ system filter bandpasses convolved with a typical coated CCD. The curves represent the expected total quantum efficiencies of the camera plus telescope on the sky. Solid curves indicate the response function without atmospheric extinction; dot-dashed curves include extinction at 1.2 air masses at the altitude of the USNO Flagstaff Station.

are available on-line.²¹ These curves, as well as the other $u'g'r'i'z'$ links from this page, will be updated as needed.

This project used 183 nights of telescope time spanning a 22 month (24 lunation) period beginning in 1998 March. The raw statistics for the success of each observing run are in Table 1, where the first two columns give the year and month of the observing session followed by the UT date. The third and fourth columns give the number of nights allocated on the telescope and the number of those nights that were clear, where “clear” is defined as no clouds having been seen in the sky by the observer for a stretch greater than 3 hours at a time. As a consequence, we collected data on some nights indicated as “clear” that later proved not to

²¹ At our $u'g'r'i'z'$ Web site, <http://home.fnal.gov/~dtucker/ugriz/index.html>.

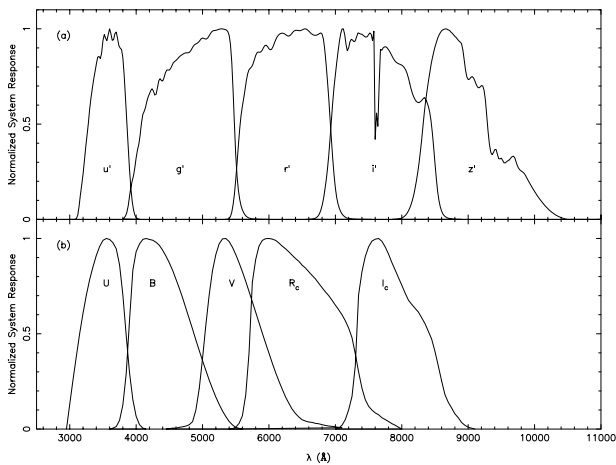


FIG. 3.—The (normalized) responses of the $u'g'r'i'z'$ system bandpasses at 1.2 air masses of extinction) compared with those of the Johnson-Morgan-Cousins ($UBVR_CI_C$) system. (Filter curves for the Johnson-Morgan UBV filters and for the Cousins R_CI_C filters were obtained from the General Catalogue of Photometric Data, at <http://obswww.unige.ch/gcpd/gcpd.html>; Mermilliod, Mermilliod, & Hauck 1997.)

TABLE 1
OBSERVING RUNS AT THE USNO 1.0 METER TELESCOPE

YYMM	UT Dates	Nights	Clear ^a	Obs.
9803	Mar 11–16	6	2	91
9804	Apr 10–17	8	2	78
9805	May 9–18	10	5	213
9806	Jun 6–14	9	6	236
9807	Jul 7–13	7	1	45
9808	Aug 5–11	7	0	0
9809	Sep 2–10	9	0	0
9810	Oct 2–8	7	3	126
9811	Oct 29–Nov 9	11	5	195
9812	Nov 28–Dec 4	7	3	70
9901	Dec 31–Jan 5	6	3	140
9902	Jan 27–Feb 4	9	6	212
9903	Feb 27–Mar 5	7	2	92
9904	Mar 27–Apr 4	9	3	130
9905	Apr 26–May 3	8	3	58
9905	May 27–31	5	0	0
9906	Jun 26–Jul 2	7	5	183
9907	Jul 23–28	6	0	0
9908	Aug 24–30	7	0	0
9909	Sep 22–28	7	4	228
9910	Oct 20–28	9	6	215
9911	Nov 18–25	8	2	97
9912	Dec 17–23	7	3	116
0001	Jan 21–27	7	0	0
Total		183	64	2525

^a Here a “clear” night is as judged at the telescope.

be usable. The last column gives the total number of usable $u'g'r'i'z'$ observations from each observing run, where one observation indicates one target field observed once in each of the five filters.

3. THE STARS AND OBSERVING STRATEGY

In order to have the standard-star system in place for the start of SDSS science operations, as required for follow-up spectroscopy target selection algorithms, it was necessary to save time during establishment of the network of standard stars. This was done by making use of previous work on standard stars so that variable stars in the initial fields were already identified. A preliminary list of 63 standard candidates was derived from the work of Thuan & Gunn (1976), Oke & Gunn (1983), and Oke (1990). This list was supplemented using the work of Sandage (1964), Veeder (1974), Stone (1977), and Kent (1985) and then pared to 36 stars using a magnitude cut. The remaining stars were then heavily supplemented using equatorial $UBVR_CI_C$ standard stars (Landolt 1973, 1983, 1992), which served to fill in gaps in right ascension and provide potential color pairs for secondary extinction terms. Additional red stars were obtained from the USNO photometry program (H. Harris 1998, private communication). At the beginning, our preliminary list contained roughly 200 candidate stars. In the end, the list was trimmed to just those stars with 10 or more observations (in each of the five filters) in the current program, or four or more observations in our program provided they had been used as standards in other systems with at least 10 observations to indicate they were not variables. In the end, 164 stars were observed often enough to be included in the reduction process for the final network. Of these, 158 were

TABLE 2
THE $u'g'r'i'z'$ FUNDAMENTAL STANDARDS

Star ^a	R.A. (J2000)	Decl. (J2000)	u'	g'	r'	i'	z'
BD +17°4708.....	22 11 30	+ 18 05 30	10.56	9.64	9.35	9.25	9.23
BD +26°2606.....	14 49 02	+ 25 42 27	10.761	9.891	9.604	9.503	9.486
..... σ			0.001	0.001	0.001	0.001	0.001
BD +21°0607.....	04 14 35	+ 22 21 06	10.289	9.395	9.114	9.025	9.017
..... σ			0.002	0.001	0.001	0.001	0.001

NOTE.—Units of right ascension are hours, minutes, and seconds, and units of declination are degrees, arcminutes, and arcseconds.

^a The magnitudes for BD +17°4708 are defined as given in this table.

retained for the final catalog of standards defining the $u'g'r'i'z'$ system.

The primary goals for the SDSS are studies of large-scale structure using galaxies and QSOs, so this first version of the standard network is limited, for the most part, to stars bluer than about M0 to avoid the strengthening metal bands and flare stars. Further, most of the survey area is around the north celestial pole with a limited area near the celestial equator, so a heavy emphasis was placed on stars in the northern hemisphere. Expansion of the network to the southern hemisphere and to redder stars is underway (see § 6).

Rather than selecting some fiducial spectral type to have null colors (as in the $UBVR_CIC$ system), our aim was to set the $u'g'r'i'z'$ standard-star network on the AB system. Recall that, in the AB system, a monochromatic magnitude is defined such that

$$\text{AB}_\nu = -2.5 \log f_\nu - 48.60 , \quad (1)$$

where f_ν is the flux per unit frequency from an object in ergs $\text{s}^{-1} \text{cm}^{-2} \text{Hz}^{-1}$; thus,

$$f_\nu(\text{Jy}) = 3631 \text{ dex}(-0.4\text{AB}_\nu) \quad (2)$$

(Oke & Gunn 1983; Fukugita et al. 1996).

As noted, the AB is, strictly speaking, a *monochromatic* system, defining a magnitude for a single frequency ν . The $u'g'r'i'z'$ system, however, is very much a *broadband* filter system. Tying a broadband system to a monochromatic flux is complicated by the existence of stellar absorption lines and by the fact that the mean wavelength of a broadband filter depends on a given star's color. As a compromise solution, we follow the lead of Fukugita et al. (1996) and define an AB *broadband* magnitude by the following equation:

$$m = -2.5 \log \frac{\int d(\log \nu) f_\nu S_\nu}{\int d(\log \nu) S_\nu} - 48.60 , \quad (3)$$

where f_ν is the energy flux per unit frequency on the atmosphere and S_ν is the system response.

To zero-point the $u'g'r'i'z'$ system, we used the synthetic AB $u'g'r'i'z'$ magnitudes of the F subdwarf BD +17°4708 as calculated by Fukugita et al. (1996). Using equation (3), Fukugita et al. computed this star's AB broadband magnitudes by convolving the $u'g'r'i'z'$ system response (Fig. 2) with the Vega-calibrated spectrophotometry of BD +17°4708. Our observations of BD +17°4708 were then forced to match these synthetic magnitudes, and all of the standard stars were scaled to this zero point. Thus there is a

formally defined relationship between $u'g'r'i'z'$ magnitudes and photon flux.

Initial estimates (D. Eisenstein 2001, private communication; D. Finkbeiner 2001, private communication) indicate that the present network deviates from a true AB broadband system by no more than about 10% in u' and z' and 5% in $g'r'i'$. These systematic errors are due to uncertainties in the absolute calibration of the synthetic $u'g'r'i'z'$ magnitudes of BD +17°4708 and include uncertainties

In the USNO filter transmissions;

In the CCD response;

In the atmospheric correction to the filter curves;

In the relative calibration of BD +17°4708 to Vega; and

In the absolute calibration of Vega.

Since the deviations from a true AB system are due to zero-point magnitude offsets in the absolute calibration of BD +17°4708 and not due to linear color shifts within the network of stars itself, future corrections toward an AB system—if warranted—should only entail a small additive constant in the standard-star magnitudes in each filter band, once these constants have been well determined.

In practice, during the early stages of this program, we needed more than one star to cover the sky for those times when BD +17°4708 was not visible, so two other F subdwarfs were chosen to be reference stars to supplement BD +17°4708: BD +26°2606 and BD +21°0607 (Table 2). BD +26°2606 has excellent spectrophotometry relative to BD +17°4708, and BD +21°0607 has excellent photometric measurements in the Thuan-Gunn system. Thus, all three of these stars were used as fundamental calibration stars during the setup of the $u'g'r'i'z'$ standard-star network. Note, however, that the final system zero point is tied solely to the synthetic photometry of BD +17°4708.

At the telescope, we tried to observe one of the three fundamental stars at least every 90 minutes to determine the zero points and judge stability for each night. In addition to the fundamental standards, the target list of primary standards was chosen to maximize the color and air-mass ranges for each night. In general, two or three primary fields were observed several times to monitor extinction manually at the telescope over the course of a night. These values were compared with the “all sky” extinction values determined later by the reduction software using all observations for the night. Additional fields were also observed in a random order to provide a good color spread near the meridian and at high air mass. We attempted to observe each of these fields two or three times a night with at least 1 hr between repeated observations. On the next usable night of the same

observing run, a different set of manual extinction fields was selected and different primary candidate fields were chosen with some, but not complete, overlap. This method reduces dependence on any particular set of extinction stars. The equatorial fields were generally used for extinction to maximize the air-mass range and leverage the effect of the color terms. The sky distribution of the final set of stars is shown in Figure 4.

Finally, typically several additional stars within each candidate field were tagged as “extra” or “monitor” stars. Although these stars were excluded from the $u'g'r'i'z'$ standard-star network, they are being calibrated in the $u'g'r'i'z'$ system and, after culling variables, will form the basis of a future catalog of supplementary $u'g'r'i'z'$ standards useful for photometric calibration of data from large-format CCD mosaic imaging cameras (Smith et al. 2002).

4. REDUCTIONS

4.1. Software

The reductions for this standard system were performed using the “monitor telescope pipeline” (`mtpipe`), a suite of code written in the SDSS software environment (Stoughton 1995; Sergey et al. 1996). For the development of the standard-star network, the pipeline reductions for each night occurred in three steps—`preMtFrames`, `mtFrames`, and `excal`—briefly described here. A more detailed description can be found in a forthcoming paper (Tucker et al. 2002).

The first package, `preMtFrames`, creates the directory structure for the reduction of a night’s data, including parameter files needed as input for the other three packages, and runs quality-assurance tests on the raw data. It identifies the image type (e.g., bias frame, twilight flat, standard field), matches the frame name to a list of approved standard-star field names, verifies that a full set of frames ($u'g'r'i'z'$) are present for each field, and creates quality-assurance histograms for the bias and flat-field frames.

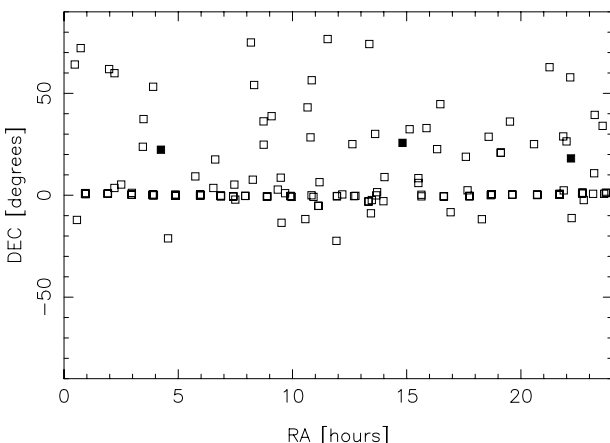


Fig. 4.—Distribution of the primary standards in right ascension and declination. Clearly seen are the clustering of stars near the celestial equator and the relative dearth of standards in the southern hemisphere. Most of the equatorial fields contain multiple stars; therefore, though there are 158 stars in the system, there are not as many individual points on this plot. The three fundamental standards—BD +17°4708, +26°2606, and +21°0607—are indicated by the filled squares.

The next package, `mtFrames`, is the image processing portion of the software. This package creates median-filtered bias and flat frames, applies them to the images, and then extracts aperture photometry on all objects found in each image. The candidate standard stars are measured in a 24"-diameter aperture. This large size was selected to avoid problems associated with defocusing the brightest stars, required for some of the observations.

The third package, `excal`, takes the output of `mtFrames` and identifies the individual primary candidate and fundamental stars within each field and then calculates the photometric zero point and the atmospheric extinction using the instrumental magnitudes for these stars as input. Before the standard-star network was calibrated, we used the candidate primary stars as extinction standards and also solved for their best-fit magnitudes based upon that night’s observations. In this mode of operation, only the three fundamental stars—BD +17°4708, +26°2606, and +21°0607—had fixed magnitudes; observations of one or more of these three set the photometric zero point for the night.

Two additional `mtpipe` packages—`solve_network` and `superExcal`—were used for the final calibration of the primary standard star network. These are similar to `excal` in that they solve for the photometric parameters of a set of data and for the best-fit magnitudes of the primary standards. They differ from `excal` in that they use a single star—BD +17°4708—to set the zero point for the photometric solution. BD +17°4708 is *defined* to have the magnitudes given in Table 2 and sets the zero point for the SDSS standard-star network. Although both `solve_network` and `superExcal` perform a similar task, they differ from each other in that `superExcal` is largely an outgrowth of the code in `excal` and its least-squares solver, but generalized to run on multiple nights of data; `solve_network`, however, was written completely independently of the `excal` code by one of us (M. W. R.). As such, `solve_network` has provided a useful independent check of our `superExcal` results.

To calibrate the standard stars, we took the following steps:

1. We ran `preMtFrames`, `mtFrames`, and `excal` on each night of data from the USNO 1.0 m telescope.
2. From the output of `excal` and from observer notes at the telescope, we determined which nights were photometric.
3. Using the output of `mtFrames` and `excal`, we ran `superExcal` for the final version of the calibrations.
4. Using the output of `mtFrames` and `excal`, we ran the `solve_network` code as an independent check of our `superExcal` results.
5. Finally, we applied a small (0.00–0.04 mag) red-leak correction to the $u'-g'$ colors, to remove the effects of the u' -filter red leaks (see § 4.3).

4.2. The Photometric Equations

The equations used to recover the $u'g'r'i'z'$ system have the form

$$u'_{\text{inst}} = u'_0 + a_u + b_u(u' - g')_0 + k_u X + c_u[(u' - g')_0 - (u' - g')_{0,zp}](X - X_{zp}), \quad (4)$$

$$g'_{\text{inst}} = g'_0 + a_g + b_g(g' - r')_0 + k_g X + c_g[(g' - r')_0 - (g' - r')_{0,zp}](X - X_{zp}), \quad (5)$$

$$\begin{aligned} r'_{\text{inst}} &= r'_0 + a_r + b_r(r'-i')_0 + k_r X \\ &\quad + c_r[(r'-i')_0 - (r'-i')_{0,\text{zp}}](X - X_{\text{zp}}), \end{aligned} \quad (6)$$

$$\begin{aligned} i'_{\text{inst}} &= i'_0 + a_i + b_i(i'-z')_0 + k_i X \\ &\quad + c_i[(i'-z')_0 - (i'-z')_{0,\text{zp}}](X - X_{\text{zp}}), \end{aligned} \quad (7)$$

$$\begin{aligned} z'_{\text{inst}} &= z'_0 + a_z + b_z(i'-z')_0 + k_z X \\ &\quad + c_z[(i'-z')_0 - (i'-z')_{0,\text{zp}}](X - X_{\text{zp}}). \end{aligned} \quad (8)$$

Taking the g' equation as an example, we note that g'_{inst} is the measured instrumental magnitude, g'_0 is the extra-atmospheric magnitude, $(g' - r')_0$ is the extra-atmospheric color, a_g is the nightly zero point, k_g is the first-order extinction coefficient, b_g is the system transform coefficient, and c_g is the second-order (color) extinction coefficient. The air mass of observation, X , is as defined by Bemporad (1904).

The zero-point constants, X_{zp} and $(g' - r')_{0,\text{zp}}$, used in the second-order extinction term, were defined respectively to be the average standard-star observation air mass $\langle X \rangle = 1.3$ and the “cosmic color,” as listed in Table 3. The cosmic color values were derived from 4428 objects with $19 < r' < 20$ in SDSS survey run 752, camera column 3, fields 11–100 (see Gunn et al. 1998 for a description of the SDSS survey camera). This area is on the celestial equator at a Galactic latitude of about 42° . The use of these zero-point constants permits setting c_g to zero without affecting the values of the other terms in the photometric equation (a_g , b_g , and k_g), thus simplifying the photometric equations for projects not requiring the highest photometric accuracy.

The `excal` and `superExcal` packages solve each of the photometric equations (eqs. [4]–[8]) iteratively, performing the following loop:

1. Feed into the equations the current estimates for the extra-atmospheric magnitudes, colors, and photometric coefficients (e.g., for eq. [5], g'_0 , r'_0 , a_g , b_g , c_g , and k_g). For the first iteration of this loop, initial estimates for these parameters are fed into the equations.

2. Solve each of the equations in turn for the extra-atmospheric magnitude and the non-color-dependent coefficients (e.g., g'_0 , a_g , and k_g), keeping the color-dependent coefficients (e.g., b_g , c_g) fixed.

3. Solve each of the equations in turn for the two color-dependent coefficients (e.g., b_g , c_g), keeping the extra-atmospheric magnitude and the non-color-dependent coefficients fixed (e.g., g'_0 , a_g , and k_g).

4. Permit the user to delete (or undelete) outliers interactively.

This loop will be performed as long as the user continues to delete (or undelete) observations interactively from the solution. (To ensure that the user has finished modifying the data set, this loop will run an additional three times after the

last user modification before outputting the final photometric solutions.)

One can also choose to fix any of the photometric coefficients to a preset value and *not* solve for it. For instance, in setting up the standard-star network, we chose to fix the system transform coefficients (e.g., b_g in eq. [5]) to zero, since the USNO 1.0 m, its CCD, and its filters are the defining instruments of the $u'g'r'i'z'$ system.

Finally, we note that equations (4)–(8), which are fitted by `excal` and `superExcal`, take the standard magnitudes and colors and convert them to instrumental magnitudes. The inverse equations are

$$\begin{aligned} u'_0 &= u'_{\text{inst}} + \hat{a}_u + \hat{b}_u(u' - g')_{\text{inst}} + \hat{k}_u X \\ &\quad + \hat{c}_u[(u' - g')_{\text{inst}} - (u' - g')_{\text{inst,zp}}](X - X_{\text{zp}}), \end{aligned} \quad (9)$$

$$\begin{aligned} g'_0 &= g'_{\text{inst}} + \hat{a}_g + \hat{b}_g(g' - r')_{\text{inst}} + \hat{k}_g X \\ &\quad + \hat{c}_g[(g' - r')_{\text{inst}} - (g' - r')_{\text{inst,zp}}](X - X_{\text{zp}}), \end{aligned} \quad (10)$$

$$\begin{aligned} r'_0 &= r'_{\text{inst}} + \hat{a}_r + \hat{b}_r(r' - i')_{\text{inst}} + \hat{k}_r X \\ &\quad + \hat{c}_r[(r' - i')_{\text{inst}} - (r' - i')_{\text{inst,zp}}](X - X_{\text{zp}}), \end{aligned} \quad (11)$$

$$\begin{aligned} i'_0 &= i'_{\text{inst}} + \hat{a}_i + \hat{b}_i(i' - z')_{\text{inst}} + \hat{k}_i X \\ &\quad + \hat{c}_i[(i' - z')_{\text{inst}} - (i' - z')_{\text{inst,zp}}](X - X_{\text{zp}}), \end{aligned} \quad (12)$$

$$\begin{aligned} z'_0 &= z'_{\text{inst}} + \hat{a}_z + \hat{b}_z(i' - z')_{\text{inst}} + \hat{k}_z X \\ &\quad + \hat{c}_z[(i' - z')_{\text{inst}} - (i' - z')_{\text{inst,zp}}](X - X_{\text{zp}}). \end{aligned} \quad (13)$$

Note that the inverse coefficients have circumflexes, indicating that they do not necessarily have the same values as the direct coefficients of equations (4)–(8). For a filter x with filter y as its color-index conjugate—i.e., filter x ’s color index is $(x-y)$ —the conversions from *direct* to *inverse* coefficients are

$$\hat{a}_x = a_x - b_x(a_x - a_y), \quad (14)$$

$$\hat{b}_x = b_x, \quad \hat{c}_x = c_x, \quad (15)$$

$$\hat{k}_x = k_x - b_x(k_x - k_y). \quad (16)$$

Again, using the SDSS g' filter as a concrete example,

$$\hat{a}_g = a_g - b_g(a_g - a_r), \quad (17)$$

$$\hat{b}_g = b_g, \quad \hat{c}_g = c_g, \quad (18)$$

$$\hat{k}_g = k_g - b_g(k_g - k_r). \quad (19)$$

Furthermore, we note that for the *inverse* equations, we must use an instrumental form of the color zero point in the second-order extinction term. Again, for a generic filter x with color index $(x-y)$,

$$(x' - y')_{\text{inst,zp}} = (x' - y')_{0,\text{zp}} + (a_x - a_y) + (k_x - k_y)X, \quad (20)$$

and for our concrete example,

$$(g' - r')_{\text{inst,zp}} = (g' - r')_{0,\text{zp}} + (a_g - a_r) + (k_g - k_r)X. \quad (21)$$

4.3. The Red-Leak Correction

There are two small red leaks associated with the u' filter—one at 8120 Å and another, larger leak beyond 10000 Å. The latter red leak is largely suppressed by the USNO

TABLE 3
THE COSMIC COLORS

Color	Value	Scatter
$u' - g'$	1.42	± 0.82
$g' - r'$	1.11	± 0.46
$r' - i'$	0.48	± 0.34
$i' - z'$	0.35	± 0.22

1.0 m CCD's low quantum efficiency at these near-infrared wavelengths.

If we define a flux sensitivity quantity, Q , by

$$Q \equiv \int d(\ln \nu) S_\nu , \quad (22)$$

where ν is the frequency and S_ν is the system quantum efficiency (Fukugita et al. 1996, eq. [5]), we can calculate the effects of the two red leaks relative to a non-red-leak u' passband. Measured for an air mass of 1.2, we find the following for the non-red-leak u' passband, the 8120 Å red leak, and the above-10000 Å red leak, respectively:

$$\begin{aligned} Q_{u'} &= 1.842 \times 10^{-2} , \\ Q_1 &= 1.009 \times 10^{-6} , \\ Q_2 &= 0.783 \times 10^{-7} . \end{aligned} \quad (23)$$

The effect of these red leaks in magnitudes can then be calculated by

$$\Delta_i = -2.5 \log (Q_i/Q_{u'}) , \quad (24)$$

where $i = 1$ or $i = 2$. We find

$$\Delta_1 = 10.654 , \quad \Delta_2 = 10.929 . \quad (25)$$

Combining these results, we can calculate the correction we need to apply to an arbitrary $u'-x'$ color of a star (where x' is an arbitrary filter) to remove the effects of these two red leaks:

$$\begin{aligned} (u'-x')_{\text{true}} &= (u'-x')_{\text{obs}} \\ &+ 2.5 \log \{1 + 0.4 \text{dex} [(u'-i')_{\text{true}} - \Delta_1] \\ &\quad + 0.4 \text{dex} [(u'-z')_{\text{true}} - \Delta_2]\} , \end{aligned} \quad (26)$$

where $(u'-x')_{\text{obs}}$ is $u'-x'$ before the red-leak correction and $(u'-x')_{\text{true}}$ is $u'-x'$ after the red-leak correction. Note that $(u'-i')_{\text{true}}$ and $(u'-z')_{\text{true}}$ are merely $(u'-x')_{\text{true}}$ for $x' = i'$ and $x' = z'$, respectively.

Note that equation (26) is an implicit equation and must be solved iteratively. Fortunately, for cases like ours in which the red-leak correction is small, we can use the following approximation:

$$\begin{aligned} (u'-x')_{\text{true}} &= (u'-x')_{\text{obs}} \\ &+ 1.086 \{\text{dex} (0.4[(u'-i')_{\text{obs}} - \Delta_1]) \\ &\quad + \text{dex} (0.4[(u'-z')_{\text{obs}} - \Delta_2])\} , \end{aligned} \quad (27)$$

where we were able to replace $(u'-i')_{\text{true}}$ with $(u'-i')_{\text{obs}}$ and $(u'-z')_{\text{true}}$ with $(u'-z')_{\text{obs}}$ as a result of the smallness of the red-leak corrections. In § 5, where we present the magnitudes and colors for the $u'g'r'i'z'$ primary standards, we use equation (27) to correct the $u'-g'$ colors.

4.4. Data

Both `excal` and `superExcal` solve for first-order extinction coefficients that vary over the course of the night; the extinction is determined for individual segments of time called “solution time blocks.” The first-order extinction coefficients for each night used in the `superExcal` photometric solution are given in Table 4. These are arranged by UT date and block (*YYMMDD-B*) with the corresponding Modified Julian Date for the midpoint of each solution time

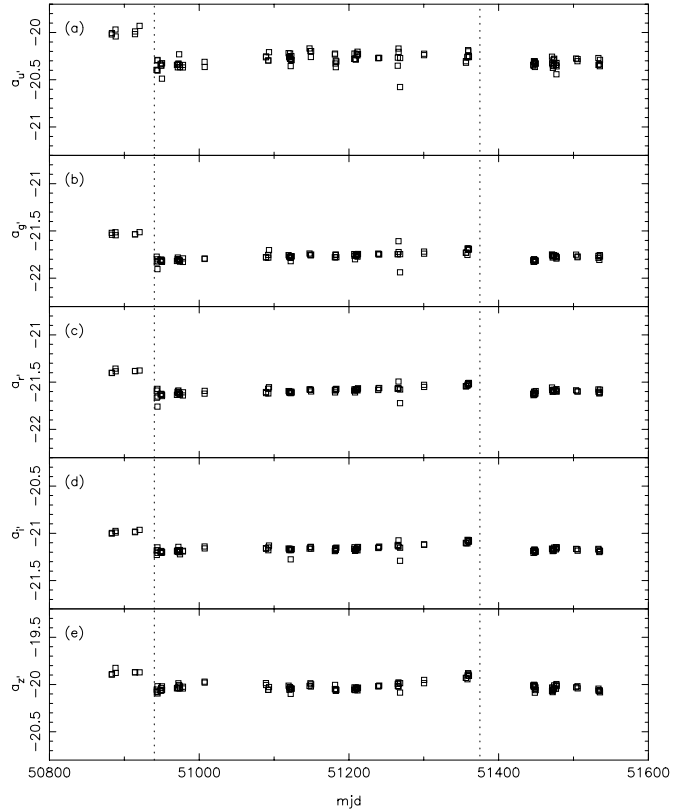


FIG. 5.—Photometric zero points calculated for each night of data used in developing the standard-star network. The mirrors were realuminized twice during our program—once after the second month of observations and again prior to the last 4 months of observations (denoted by the dotted vertical lines). The first realuminization is clearly visible as a break in the zero-point values, while the second break is less obvious. The two large gaps (approximately MJD 51,000–51,100 and 51,350–51,450) correspond to the two monsoon seasons (summers) in northern Arizona.

block, rounded to the nearest 0.01 days.²² These are listed in the first two columns of the table. The extinction coefficients and associated uncertainties are given in the remaining columns. These values were determined as part of the `superExcal` solution. The default solution block within `superExcal` was set at 3 hr. Each night was examined for obvious breaks—east versus west, the Moon, breaks around possible clouds, before and after midnight—and these were given priority for dividing the night into reduction blocks. In the absence of obvious breaks, the default solution block within `mtpipe`, 3 hr, was used. Further, each block had to contain a minimum of 10 observations per passband (about 1.5 hr observing time), after all rejections, to be kept in the final solution. In the end, 109 usable blocks on 61 nights were determined to be photometric and contained the minimum number of observations to be included in the system solution.

The zero points for each of the 61 usable nights are shown in Figure 5. These are calculated by `superExcal` once for each block of time, from fundamental standard observations. As shown, most nights have similar zero points. Clearly seen in the figure are the times when the mirrors

²² The Modified Julian Date is defined by the relation $MJD \equiv JD - 2,400,000.5$, where JD is the Julian Date.

TABLE 4
FIRST-ORDER EXTINCTION COEFFICIENTS

<i>YYMMDD-B</i>	Midpoint (MJD)	$k_{u'}$	$\sigma_{u'}$	$k_{g'}$	$\sigma_{g'}$	$k_{r'}$	$\sigma_{r'}$	$k_{i'}$	$\sigma_{i'}$	$k_{z'}$	$\sigma_{z'}$
980311-0	50,883.22	0.565	0.018	0.161	0.007	0.102	0.006	0.062	0.007	0.050	0.011
980311-1	50,883.42	0.554	0.024	0.166	0.009	0.108	0.008	0.060	0.009	0.049	0.015
980316-0	50,888.27	0.594	0.013	0.182	0.004	0.092	0.004	0.071	0.006	0.051	0.009
980316-1	50,888.44	0.617	0.017	0.188	0.007	0.105	0.006	0.075	0.007	0.071	0.012
980411-0	50,914.21	0.619	0.014	0.205	0.005	0.116	0.004	0.082	0.006	0.064	0.010
980411-1	50,914.41	0.587	0.013	0.201	0.005	0.113	0.004	0.080	0.006	0.065	0.010
980417-0	50,920.42	0.569	0.040	0.192	0.015	0.116	0.013	0.066	0.014	0.072	0.023
980510-0	50,943.24	0.769	0.017	0.264	0.007	0.177	0.006	0.149	0.007	0.167	0.010
980510-1	50,943.41	0.726	0.017	0.293	0.006	0.212	0.005	0.167	0.007	0.171	0.011
980511-0	50,944.21	0.654	0.022	0.273	0.010	0.153	0.008	0.110	0.010	0.127	0.013
980511-1	50,944.31	0.616	0.022	0.319	0.010	0.255	0.010	0.093	0.009	0.112	0.012
980511-2	50,944.43	0.682	0.022	0.236	0.008	0.158	0.007	0.099	0.009	0.113	0.014
980515-0	50,948.39	0.568	0.019	0.180	0.007	0.104	0.007	0.075	0.008	0.076	0.012
980516-0	50,949.21	0.592	0.022	0.196	0.008	0.112	0.007	0.071	0.008	0.068	0.013
980516-1	50,949.36	0.592	0.024	0.189	0.009	0.117	0.008	0.076	0.009	0.078	0.014
980517-0	50,950.27	0.656	0.031	0.187	0.008	0.123	0.007	0.082	0.008	0.036	0.013
980517-1	50,950.40	0.526	0.031	0.168	0.012	0.108	0.011	0.072	0.011	0.067	0.017
980606-0	50,970.34	0.571	0.017	0.198	0.006	0.132	0.005	0.095	0.008	0.105	0.012
980607-0	50,971.23	0.565	0.019	0.184	0.006	0.110	0.005	0.085	0.007	0.086	0.011
980607-1	50,971.38	0.585	0.018	0.180	0.007	0.117	0.006	0.094	0.008	0.073	0.012
980608-0	50,972.22	0.589	0.018	0.201	0.006	0.107	0.006	0.059	0.007	0.052	0.011
980608-1	50,972.38	0.582	0.015	0.202	0.006	0.127	0.005	0.094	0.007	0.091	0.010
980609-0	50,973.29	0.505	0.027	0.202	0.010	0.125	0.009	0.111	0.012	0.095	0.018
980610-0	50,974.23	0.597	0.019	0.207	0.008	0.134	0.007	0.086	0.008	0.092	0.012
980610-1	50,974.39	0.609	0.017	0.209	0.007	0.137	0.006	0.119	0.007	0.102	0.012
980614-0	50,978.24	0.596	0.018	0.207	0.007	0.132	0.006	0.091	0.008	0.089	0.012
980614-1	50,978.40	0.569	0.018	0.166	0.007	0.098	0.006	0.078	0.007	0.073	0.011
980713-0	51,007.22	0.566	0.029	0.191	0.009	0.130	0.007	0.074	0.009	0.067	0.014
980713-1	51,007.37	0.609	0.015	0.192	0.005	0.108	0.005	0.086	0.007	0.073	0.010
981003-0	51,089.16	0.546	0.023	0.165	0.008	0.102	0.007	0.064	0.009	0.057	0.014
981003-1	51,089.37	0.525	0.023	0.165	0.009	0.107	0.008	0.068	0.010	0.069	0.015
981006-0	51,092.20	0.572	0.017	0.169	0.006	0.088	0.006	0.059	0.007	0.066	0.011
981006-1	51,092.42	0.555	0.015	0.171	0.006	0.106	0.005	0.063	0.007	0.056	0.010
981007-0	51,093.26	0.548	0.025	0.152	0.008	0.085	0.007	0.055	0.009	0.078	0.013
981102-0	51,119.44	0.562	0.017	0.180	0.006	0.105	0.005	0.069	0.007	0.069	0.011
981103-0	51,120.42	0.544	0.015	0.160	0.005	0.097	0.005	0.067	0.006	0.077	0.010
981104-0	51,121.14	0.532	0.017	0.164	0.006	0.091	0.006	0.065	0.007	0.064	0.011
981104-1	51,121.30	0.551	0.016	0.165	0.006	0.093	0.005	0.062	0.007	0.061	0.011
981104-2	51,121.46	0.509	0.020	0.162	0.008	0.099	0.007	0.056	0.008	0.065	0.013
981105-0	51,122.27	0.611	0.016	0.194	0.007	0.100	0.006	0.143	0.008	0.118	0.012
981105-1	51,122.45	0.559	0.029	0.169	0.011	0.090	0.010	0.068	0.011	0.078	0.017
981106-0	51,123.16	0.544	0.021	0.163	0.008	0.094	0.007	0.062	0.008	0.069	0.012
981106-1	51,123.45	0.566	0.016	0.161	0.006	0.099	0.005	0.053	0.007	0.051	0.011
981130-0	51,147.42	0.495	0.018	0.150	0.007	0.082	0.006	0.061	0.008	0.058	0.012
981201-0	51,148.46	0.510	0.023	0.145	0.008	0.076	0.007	0.051	0.009	0.053	0.014
981201-0	51,149.49	0.549	0.028	0.165	0.010	0.103	0.009	0.076	0.011	0.074	0.017
981202-1	51,149.12	0.568	0.022	0.152	0.008	0.077	0.008	0.046	0.008	0.072	0.013
990103-0	51,181.24	0.527	0.019	0.172	0.006	0.092	0.006	0.071	0.007	0.047	0.011
990103-1	51,181.46	0.524	0.021	0.173	0.007	0.111	0.006	0.055	0.008	0.048	0.012
990104-0	51,182.14	0.587	0.015	0.162	0.006	0.091	0.005	0.064	0.007	0.044	0.010
990104-1	51,182.30	0.581	0.025	0.162	0.008	0.097	0.008	0.054	0.008	0.052	0.014
990104-2	51,182.49	0.625	0.029	0.156	0.011	0.087	0.025	0.063	0.011	0.056	0.016
990105-0	51,183.26	0.577	0.019	0.170	0.007	0.081	0.006	0.049	0.007	0.064	0.011
990129-0	51,207.14	0.551	0.019	0.146	0.007	0.093	0.006	0.048	0.008	0.041	0.012
990129-1	51,207.36	0.513	0.019	0.163	0.007	0.085	0.006	0.038	0.008	0.028	0.012
990130-0	51,208.15	0.542	0.019	0.186	0.007	0.106	0.007	0.064	0.008	0.058	0.012
990131-0	51,209.12	0.556	0.019	0.153	0.007	0.080	0.006	0.062	0.008	0.048	0.012
990201-0	51,210.20	0.541	0.015	0.170	0.005	0.107	0.004	0.070	0.006	0.061	0.010
990202-0	51,211.22	0.548	0.014	0.166	0.005	0.092	0.005	0.050	0.006	0.046	0.010
990202-1	51,211.47	0.518	0.028	0.178	0.011	0.105	0.009	0.069	0.010	0.056	0.016
990203-0	51,212.18	0.516	0.021	0.151	0.008	0.082	0.007	0.046	0.008	0.051	0.013
990302-0	51,239.21	0.557	0.016	0.177	0.006	0.125	0.006	0.079	0.007	0.068	0.010
990302-1	51,239.43	0.542	0.016	0.173	0.006	0.103	0.005	0.079	0.007	0.061	0.011
990303-0	51,240.44	0.535	0.017	0.166	0.006	0.093	0.006	0.060	0.007	0.047	0.011

TABLE 4—Continued

<i>YYMMDD-B</i>	Midpoint (MJD)	$k_{u'}$	$\sigma_{u'}$	$k_{g'}$	$\sigma_{g'}$	$k_{r'}$	$\sigma_{r'}$	$k_{i'}$	$\sigma_{i'}$	$k_{z'}$	$\sigma_{z'}$
990328-0	51,265.16	0.696	0.022	0.241	0.008	0.156	0.007	0.100	0.008	0.104	0.012
990328-1	51,265.35	0.622	0.020	0.221	0.007	0.143	0.007	0.098	0.008	0.104	0.012
990329-0	51,266.17	0.740	0.023	0.258	0.009	0.175	0.007	0.113	0.008	0.121	0.012
990329-1	51,266.38	0.802	0.019	0.375	0.006	0.253	0.005	0.174	0.007	0.157	0.011
990331-0	51,268.22	1.160	0.023	0.575	0.010	0.403	0.008	0.323	0.009	0.232	0.013
990331-1	51,268.43	0.735	0.022	0.305	0.008	0.203	0.007	0.147	0.009	0.100	0.014
990502-0	51,300.30	0.620	0.017	0.212	0.006	0.129	0.008	0.100	0.007	0.109	0.011
990502-1	51,300.42	0.608	0.033	0.223	0.013	0.143	0.010	0.099	0.012	0.068	0.019
990627-0	51,356.22	0.601	0.021	0.179	0.007	0.116	0.007	0.090	0.008	0.109	0.012
990627-1	51,356.39	0.610	0.015	0.176	0.006	0.114	0.005	0.089	0.007	0.105	0.011
990629-0	51,358.24	0.583	0.016	0.205	0.006	0.119	0.006	0.091	0.007	0.107	0.011
990629-1	51,358.41	0.557	0.017	0.139	0.006	0.099	0.006	0.045	0.007	0.047	0.011
990630-0	51,359.23	0.561	0.024	0.189	0.009	0.118	0.008	0.088	0.009	0.074	0.014
990630-1	51,359.40	0.572	0.019	0.179	0.007	0.115	0.007	0.087	0.008	0.076	0.012
990701-0	51,360.23	0.637	0.017	0.204	0.006	0.132	0.006	0.095	0.007	0.107	0.011
990701-1	51,360.39	0.634	0.017	0.197	0.006	0.129	0.006	0.094	0.007	0.097	0.011
990925-0	51,446.27	0.584	0.016	0.162	0.006	0.098	0.005	0.077	0.007	0.091	0.010
990925-1	51,446.45	0.590	0.016	0.176	0.006	0.110	0.005	0.091	0.007	0.099	0.010
990926-0	51,447.16	0.562	0.016	0.178	0.006	0.094	0.005	0.072	0.007	0.076	0.010
990926-1	51,447.31	0.546	0.022	0.174	0.009	0.087	0.008	0.056	0.009	0.073	0.014
990926-2	51,447.45	0.554	0.016	0.158	0.006	0.082	0.005	0.063	0.007	0.062	0.011
990927-0	51,448.17	0.553	0.016	0.164	0.006	0.093	0.005	0.061	0.007	0.059	0.011
990927-1	51,448.32	0.589	0.020	0.170	0.008	0.106	0.007	0.075	0.008	0.099	0.012
990927-2	51,448.45	0.550	0.017	0.178	0.006	0.107	0.006	0.071	0.007	0.086	0.011
990928-0	51,449.18	0.583	0.016	0.180	0.006	0.108	0.006	0.076	0.007	0.087	0.011
990928-1	51,449.42	0.557	0.017	0.173	0.006	0.084	0.006	0.074	0.007	0.078	0.011
991020-0	51,471.20	0.539	0.043	0.166	0.016	0.086	0.014	0.065	0.016	0.092	0.024
991020-1	51,471.44	0.578	0.020	0.166	0.006	0.093	0.005	0.063	0.007	0.057	0.011
991021-0	51,472.17	0.591	0.014	0.182	0.006	0.110	0.004	0.077	0.006	0.081	0.010
991021-1	51,472.34	0.604	0.020	0.167	0.008	0.098	0.007	0.061	0.008	0.053	0.013
991022-0	51,473.12	0.557	0.021	0.167	0.008	0.100	0.007	0.068	0.008	0.055	0.013
991022-1	51,473.48	0.569	0.031	0.153	0.012	0.095	0.010	0.072	0.012	0.050	0.018
991023-0	51,474.14	0.546	0.018	0.167	0.007	0.094	0.006	0.056	0.007	0.047	0.011
991023-1	51,474.30	0.581	0.020	0.174	0.008	0.097	0.007	0.065	0.008	0.067	0.012
991025-0	51,476.47	0.591	0.026	0.168	0.009	0.099	0.008	0.071	0.010	0.084	0.015
991026-0	51,477.16	0.702	0.028	0.210	0.011	0.121	0.010	0.069	0.011	0.061	0.016
991026-1	51,477.30	0.617	0.019	0.194	0.008	0.105	0.007	0.067	0.008	0.067	0.012
991026-2	51,477.46	0.673	0.022	0.222	0.008	0.136	0.007	0.086	0.009	0.080	0.013
991121-0	51,503.38	0.549	0.016	0.157	0.005	0.094	0.005	0.060	0.007	0.061	0.010
991123-0	51,505.20	0.569	0.017	0.180	0.006	0.105	0.006	0.056	0.007	0.025	0.012
991123-1	51,505.45	0.530	0.021	0.164	0.008	0.096	0.007	0.060	0.009	0.029	0.013
991221-0	51,533.16	0.526	0.014	0.157	0.005	0.087	0.005	0.054	0.006	0.064	0.010
991221-1	51,533.37	0.577	0.019	0.175	0.007	0.104	0.006	0.064	0.008	0.062	0.013
991222-0	51,534.49	0.591	0.022	0.200	0.009	0.122	0.008	0.085	0.009	0.074	0.014
991223-0	51,535.14	0.585	0.023	0.153	0.009	0.109	0.008	0.067	0.009	0.063	0.015
991223-1	51,535.31	0.536	0.018	0.164	0.007	0.090	0.006	0.070	0.008	0.079	0.011

were realuminized: once after the second month and again prior to the last 4 months of observations. A few outlying points correspond to high extinction values, but the derived magnitudes for these nights are within the 2σ error limits for stars observed on those nights.

The primary extinction coefficients (Table 4) for each block are plotted in Figure 6. As seen, the extinction values were generally stable during the program. Three nights with higher than normal extinction values (and low zero points) are seen. However, as mentioned above, the final magnitude values for each of the stars observed during these times were within the accepted limits.

Secondary extinction (color term) values are given in Table 5. Calculating these values is an option in the pipeline code. For the system setup, we assumed there would be one

fixed value for all nights and solved for these coefficients. This correction is minor compared with the primary extinction terms, so our assumption of a single value does not impact the solution. (For comparison, we also list the values for the secondary extinction coefficients obtained by `solve_network`.)

The residuals of each observation in the network solution were examined for trends, as a function of several different variables, within the final network solution. The plots of these test results are available on our $u'g'r'i'z'$ Web site. To summarize, we found no apparent trends in the residuals as a function of

Time (over the course of the program);
Air mass;
Magnitude;

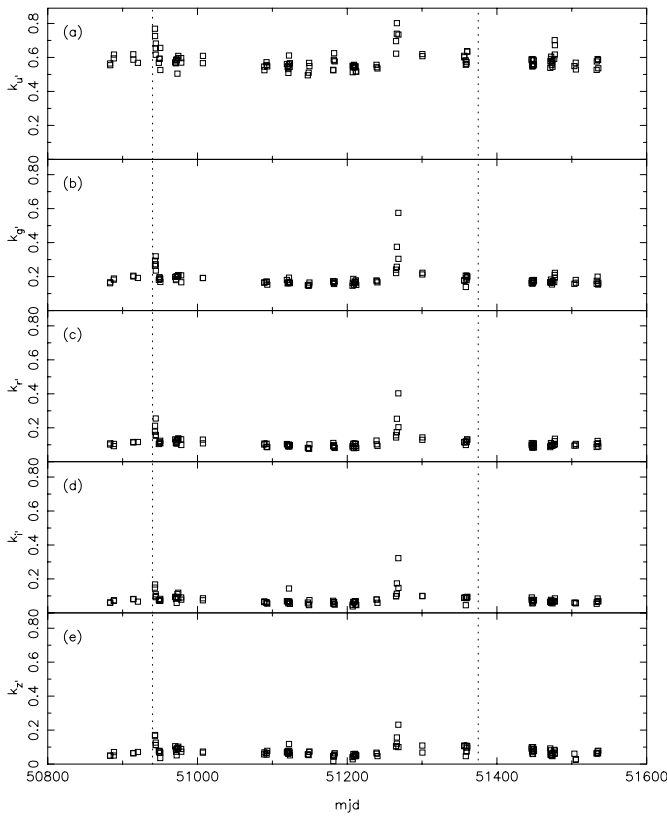


FIG. 6.—Primary extinction coefficients for each block of data used in developing the standard-star network. The five nights with high extinction values (MJD 50,943, 51,265, 51,266, 51,268, and 51,477) correspond to the nights with low zero points. The times when the mirror was realuminized are denoted by the two dotted vertical lines.

Color;
Product of color and air mass;
Right ascension;
Declination;
Hour angle; or
Ambient temperature of observation.

We did see an increase in the scatter of the residuals in the u' filter at fainter magnitudes and for redder stars. This was caused by the tailored exposure times used on each field with multiple candidate stars. Since the exposure times for each standard field were tailored for the brightest candidate, the second, third, fourth, etc., star in each field will be increasingly underexposed, resulting in the scatter. We also noticed an increase in scatter for the bluer star residuals in the z' filter, also an artifact of the tailored exposure lengths.

The above tests—those showing the residuals from individual observations plotted against a variety of variables—

TABLE 5
SECOND-ORDER EXTINCTION COEFFICIENTS

Filter	superExcal	solve_network
$c_{u'}$	-0.021 ± 0.003	-0.032
$c_{g'}$	-0.016 ± 0.003	-0.015
$c_{r'}$	-0.004 ± 0.003	$+0.000$
$c_{i'}$	$+0.006 \pm 0.003$	$+0.005$
$c_{z'}$	$+0.003 \pm 0.003$	$+0.006$

TABLE 6
MEAN ERRORS IN CALIBRATED MAGNITUDES

FILTER	SURVEY GOAL	CALCULATED		
		Minimum	Average	Maximum
$\sigma_{u'}$	0.015	0.001	0.007	0.025
$\sigma_{g'}$	0.010	0.001	0.002	0.006
$\sigma_{r'}$	0.010	0.001	0.002	0.008
$\sigma_{i'}$	0.010	0.001	0.002	0.009
$\sigma_{z'}$	0.015	0.001	0.003	0.016

were useful in showing that there are no obvious systematic trends in the $u'g'r'i'z'$ primary standard star network. To examine the systemwide rms errors in the network, we have plotted the standard error of the mean magnitude for each star in Figures 7 and 8. We have also listed the minimum, the average, and the maximum of these “per star” errors in Table 6, along with the goals needed to meet the survey end-to-end requirements. Figure 7 shows the mean error as a function of magnitude. We clearly see in this plot that the fainter standards in each multiple-star field, generally the equatorial fields, have higher errors. Figure 8 shows the mean error as a function of color. Again, we see an increase in the error for the fainter stars in each multiple-star field, only this time the errors increase for the red stars in the u' frames and the blue stars in the z' frames. In both these plots, the horizontal dotted lines indicate the survey error

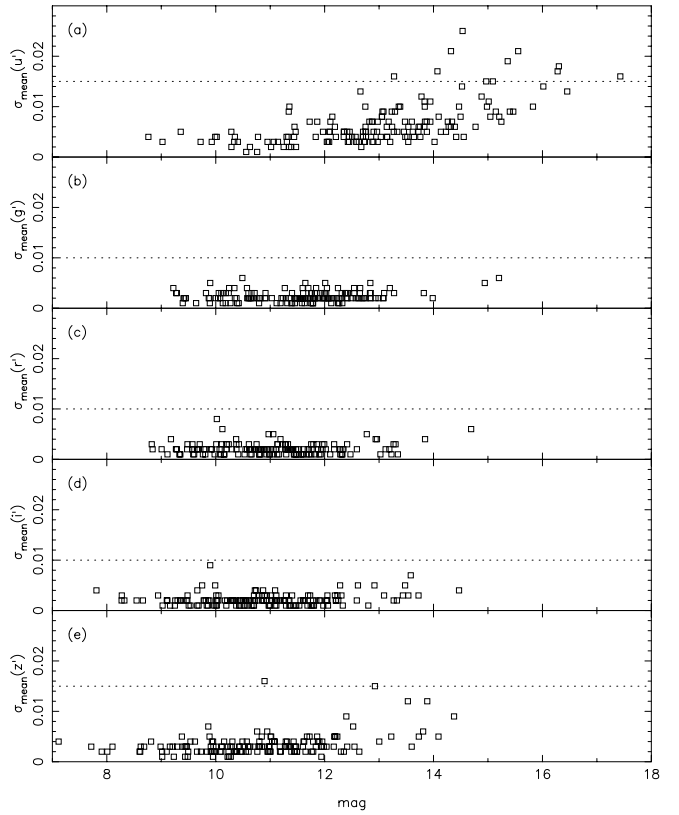


FIG. 7.—Mean error vs. magnitude [$\sigma_{\text{mean}}(u')$ vs. u' , $\sigma_{\text{mean}}(g')$ vs. g' , $\sigma_{\text{mean}}(r')$ vs. r' , $\sigma_{\text{mean}}(i')$ vs. i' , $\sigma_{\text{mean}}(z')$ vs. z']. The horizontal dotted lines are the survey requirements for the standard network to meet.

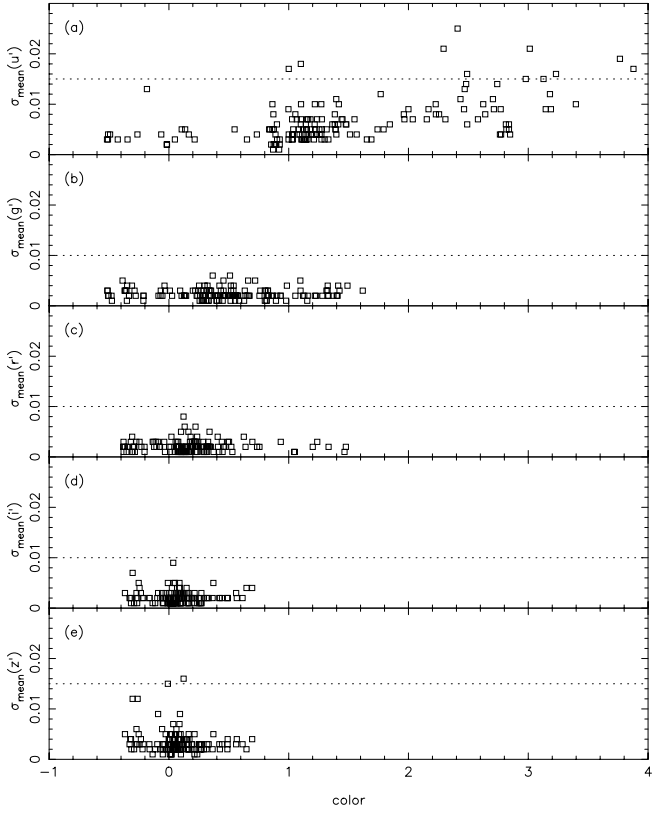


FIG. 8.—Mean error vs. color [$\sigma_{\text{mean}}(u')$ vs. $u'-g'$, $\sigma_{\text{mean}}(g')$ vs. $g'-r'$, $\sigma_{\text{mean}}(r')$ vs. $r'-i'$, $\sigma_{\text{mean}}(i')$ vs. $i'-z'$, $\sigma_{\text{mean}}(z')$ vs. $z'-z'$]. The horizontal dotted lines are the survey requirements for the standard network to meet.

budget allotted to the standard-star network (the survey goals from Table 6). Note that for all but a handful of stars in u' and z' , we more than satisfy the survey goals.

The distribution of the stars in R.A.-($g'-r'$) color space is shown in Figure 9. While this plot was generally used as an observation planning tool during system development, it

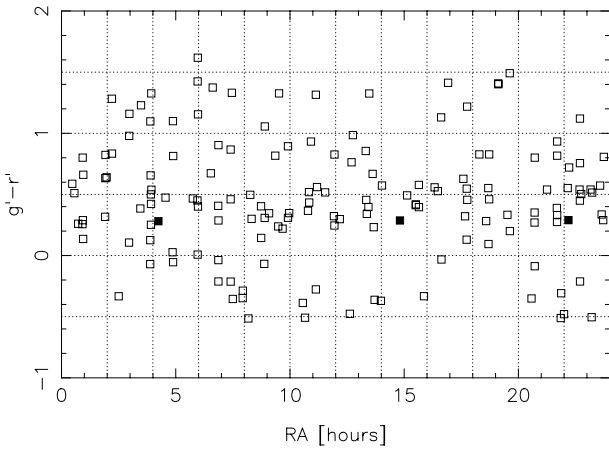


FIG. 9.—Distribution in $g'-r'$ vs. right ascension space for the 158 $u'g'r'i'z'$ primary and fundamental standards (the three filled squares mark the positions of the three fundamental standards). Grid lines demarcate boxes 0.5 mag wide in $g'-r'$ and 2^h wide in right ascension. Note that almost each box in the range $-0.5 < g'-r' < 1.5$ contains one or more standard stars.

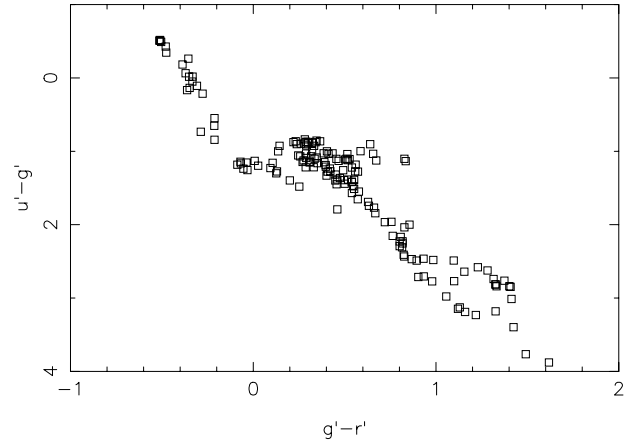


FIG. 10.—The $u'-g'$ vs. $g'-r'$ color-color plot for the 158 $u'g'r'i'z'$ standard stars.

does show the generally uniform distribution of the standards around the sky, at least in the northern hemisphere.

The color-color space distributions of the final set of stars are shown in Figure 10 ($u'-g'$ vs. $g'-r'$), Figure 11 ($g'-r'$ vs. $r'-i'$), and Figure 12 ($r'-i'$ vs. $i'-z'$). The break in the linear color transforms at about spectral type M0 is clearly seen in Figure 11 and is also evident in Figure 12. Separation of the metal-poor stars from the main-sequence dwarfs is seen in Figure 10. The clump of stars in the blue-blue corner of all three of these plots are the warm-hot white dwarfs

Approximate relations for transforming magnitudes and colors from the Johnson-Morgan-Cousins $UBVR_{\text{C}}I_{\text{C}}$ system to the SDSS $u'g'r'i'z'$ system were given in the system-defining paper (Fukugita et al. 1996). Full details of the development of the relations presented herein are given by Jorgensen et al. (2002). Fukugita et al.'s (1996) synthetic transformations and our observed relationships are given in Table 7. Our observed transformation relationships are also shown in graphical form in Figure 13 and are similar to those of Fukugita et al. (their Fig. 6). We also present relations for the inverse transformations—from $u'g'r'i'z'$ to $UBVR_{\text{C}}I_{\text{C}}$ —in Table 7 and in Figure 14.

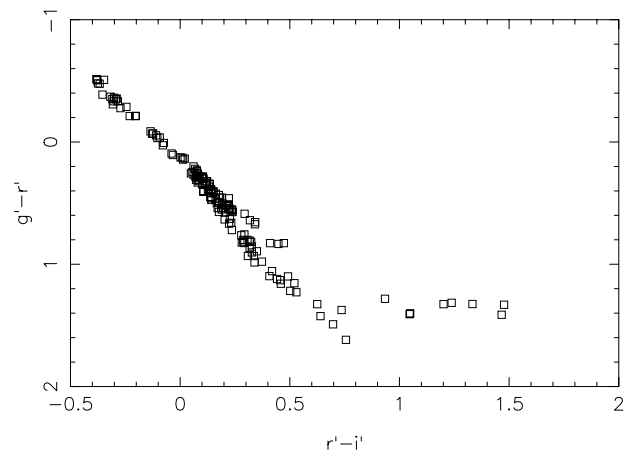


FIG. 11.—The $g'-r'$ vs. $r'-i'$ color-color plot for the 158 $u'g'r'i'z'$ standard stars.

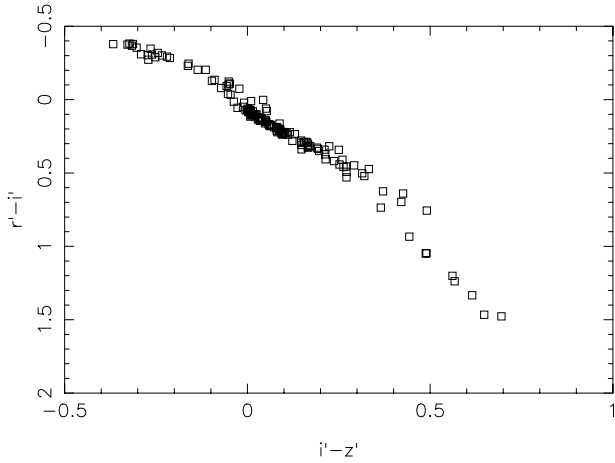


FIG. 12.—The $r' - i'$ vs. $i' - z'$ color-color plot for the 158 $u'g'r'i'z'$ standard stars.

5. THE STANDARD-STAR NETWORK

Finally, we present the magnitude and color data for each star along with astrometric, proper-motion, and spectroscopic information. Table 8 is arranged in order of increasing right ascension and contains the star name, right ascension, and declination (J2000) in the first three columns. The next five columns give the r' magnitudes and the four color indexes. (Note that the $u' - g'$ colors listed here have had the u' red-leak correction of eq. [27] applied; see Fig. 15.) These five columns are linked with the next five columns, which give the standard deviation of the measurements. As a note, during the reductions we calculated the five filter magnitudes. We report colors here as an observational aid. The associated uncertainties for the colors are derived from the magnitude errors added in quadrature. As such, they may be slightly overestimated. The last five col-

umns of this table give the number of individual measurements, by filter, that were used to determine the final magnitudes.

Table 9 is arranged by increasing right ascension, and the first three columns are the same as in Table 8. Column (4) gives the Guide Star Catalog (Lasker, Russel, & Jenkner 1999) or *Hipparcos* Catalogue number, or indicates that it is in the Tycho database. The coordinate epoch follows in column (5). Columns (6)–(10) give the proper motions and uncertainties in milliarcseconds per year and the reference from which these were obtained. Columns (11) and (12) give the spectral type (where known) and a reference. The last column indicates that additional notes on a star may be found at the end of the table.

6. FUTURE WORK

Though the setup of the initial primary standard stars for the $u'g'r'i'z'$ system is now complete, there is still a large amount of work remaining to make this system widely useful to the astronomical community. Two efforts that will continue through the life of the SDSS are reducing the errors in the mean magnitudes of each standard star and obtaining good magnitudes for all of the additional stars in each of the standard-star fields. These will be done by making use of the observations from the SDSS photometric monitoring telescope at Apache Point Observatory. This telescope operates every night during survey operations to obtain extinction data for survey calibration and to transfer the standard-star system, through fainter stars, to the 2.5 m survey data.

In addition to the continued refinement of the primary standard star network, two additional areas that require more work are extending the system to redder stars and to the southern hemisphere. The initial standard system was limited to stars generally bluer than about dM0, so the redder stars are needed to obtain accurate magnitudes for the

TABLE 7
TRANSFORMATIONS BETWEEN $UBVR_C I_C$ AND $u'g'r'i'z'$

Magnitude/Color	Observed	Synthetic ^a
$UBVR_C I_C$ to $u'g'r'i'z'$		
g'	$= V + 0.54(B-V) - 0.07$	$= V + 0.56(B-V) - 0.12$
r'	$= V - 0.44(B-V) + 0.12$	$= V - 0.49(B-V) + 0.11$
r' for $V-R < 1.00$	$= V - 0.81(V-R) + 0.13$	$= V - 0.84(V-R) + 0.13$
r' for $V-R \geq 1.00$	$= V - 0.84(V-R) + 0.13$
$u' - g'$	$= 1.33(U-B) + 1.12$	$= 1.38(U-B) + 1.14$
$g' - r'$	$= 0.98(B-V) - 0.19$	$= 1.05(B-V) - 0.23$
$r' - i'$ for $R-I < 1.15$...	$= 1.00(R-I) - 0.21$	$= 0.98(R-I) - 0.23$
$r' - i'$ for $R-I \geq 1.15$...	$= 1.42(R-I) - 0.69$	$= 1.40(R-I) - 0.72$
$r' - z'$ for $R-I < 1.65$...	$= 1.65(R-I) - 0.38$	$= 1.59(R-I) - 0.40$
$r' - z'$ for $R-I \geq 1.65$...	None observed	$= 2.64(R-I) - 2.16$
$u'g'r'i'z'$ to $UBVR_C I_C$		
B	$= g' + 0.47(g' - r') + 0.17$...
V	$= g' - 0.55(g' - r') - 0.03$...
$U-B$	$= 0.75(u' - g') - 0.83$...
$B-V$	$= 1.02(g' - r') + 0.20$...
$V-R$	$= 0.59(g' - r') + 0.11$...
$R-I$ for $r' - i' < 0.95$...	$= 1.00(r' - i') + 0.21$...
$R-I$ for $r' - i' \geq 0.95$...	$= 0.70(r' - i') + 0.49$...

^a From Fukugita et al. 1996.

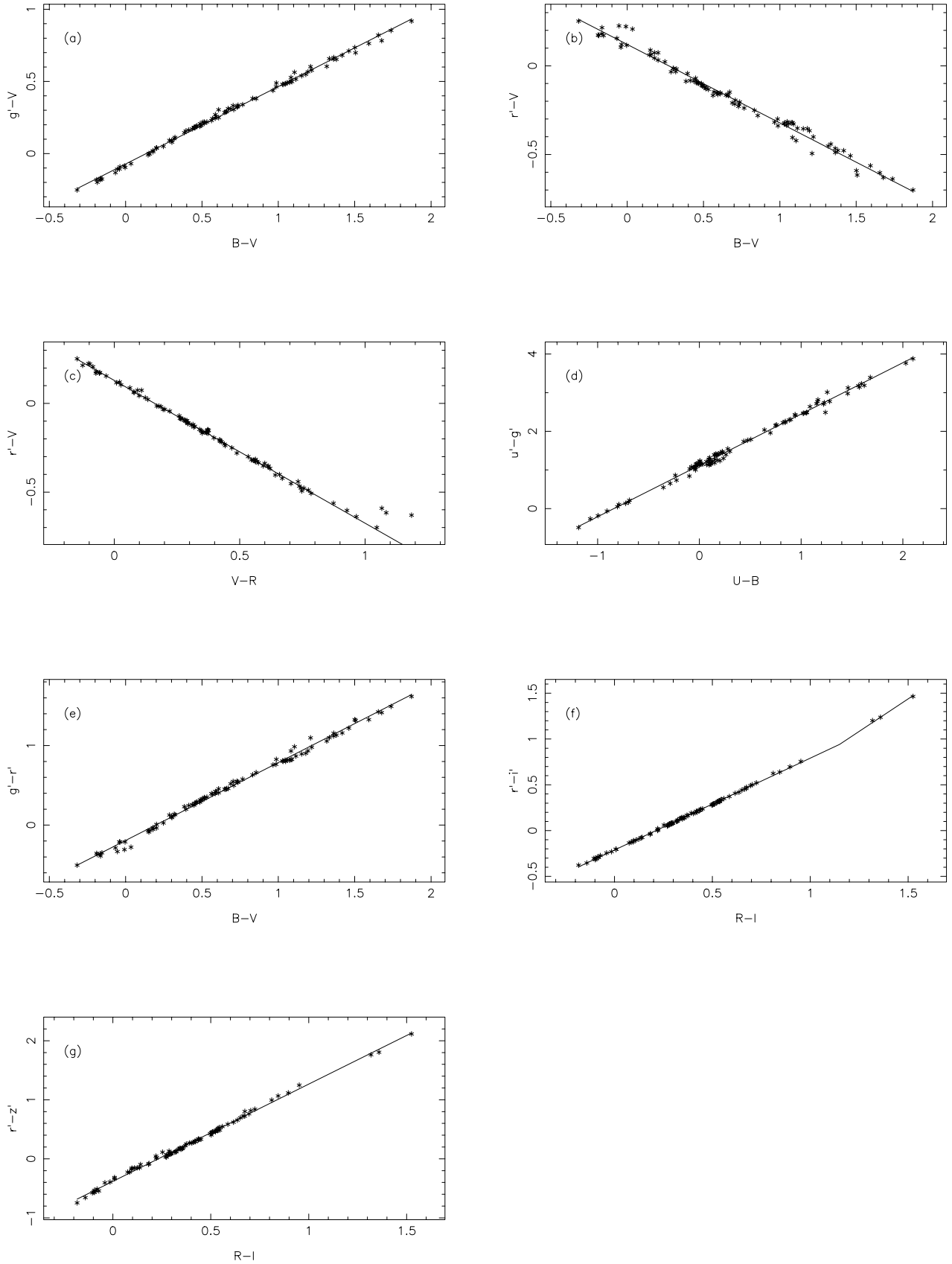


FIG. 13.—Comparison of $u'g'r'i'z'$ and $UBVR_CI_C$ magnitudes for those $u'g'r'i'z'$ standards measured by Landolt. The solid lines denote the linear fits listed under the “Observed” column of Table 7 for the $UBVR_CI_C$ -to- $u'g'r'i'z'$ transformations.

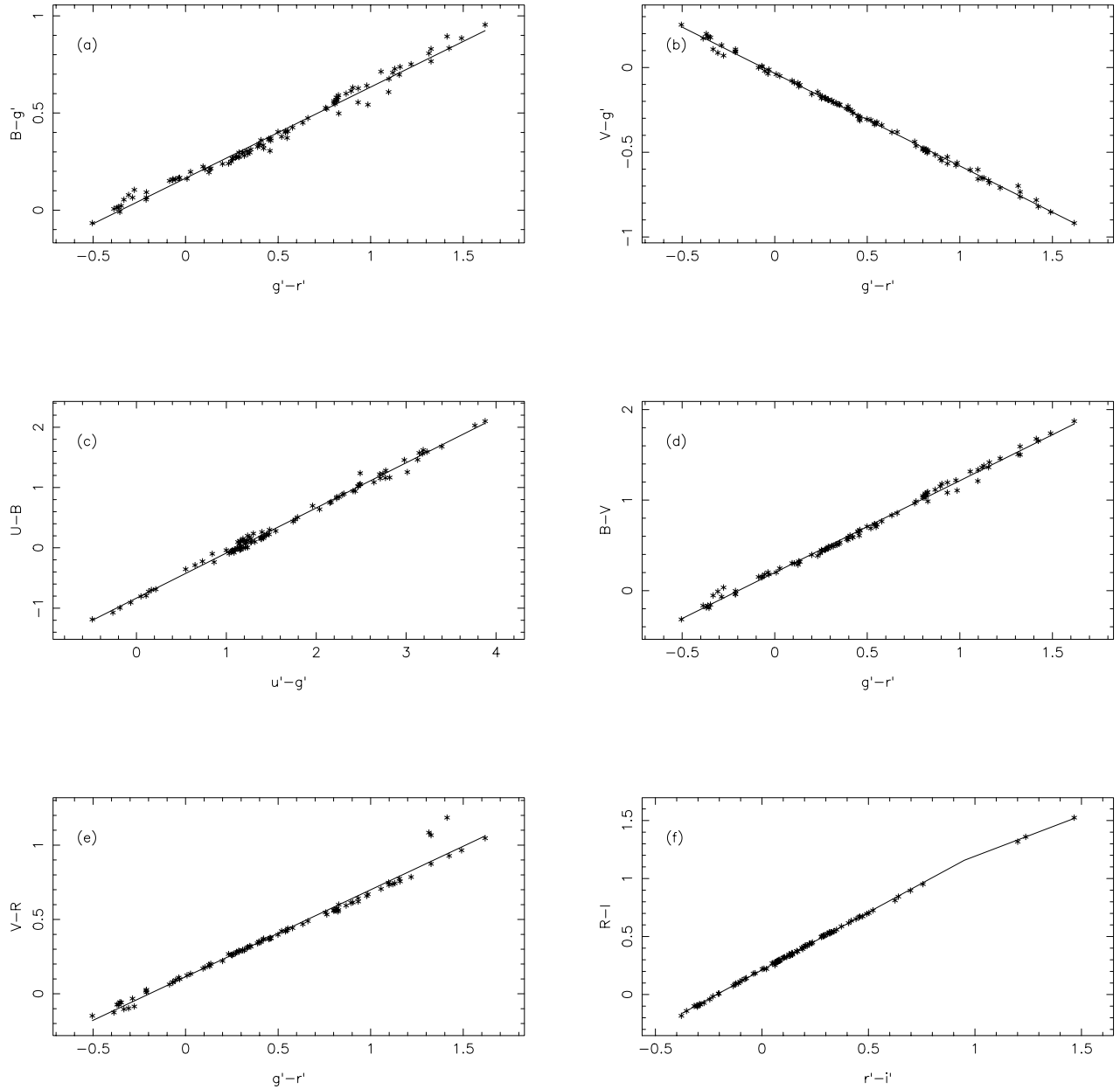


FIG. 14.—Comparison of $u'g'r'i'z'$ and $UBVR_CI_C$ magnitudes for those $u'g'r'i'z'$ standards measured by Landolt. The solid lines denote the linear fits listed under the “Observed” column of Table 7 for the $u'g'r'i'z'$ -to- $UBVR_CI_C$ transformations.

late M dwarfs and the new spectral classes, L and T. An extension to redder stars will make the logical tie into the Two Micron All Sky Survey for the redder objects more meaningful. We are developing a program to make this extension, specifically, to look for additional “knees” in the color-color diagrams. The second area of expansion is into the southern hemisphere. We began this effort in 2000 September using the 0.9 m telescope at Cerro Tololo Inter-American Observatory and the same observers and reduction software as used in the setup of the network described in the present paper.²³ We undertook this effort to minimize any discrepancies such as those that have crept into the existing $UBVR_CI_C$ standards, in which several independent

investigators have been involved in calibrating standard stars.

The Sloan Digital Sky Survey is a joint project of the University of Chicago, Fermilab, the Institute for Advanced Study, the Japan Participation Group, Johns Hopkins University, the Max-Planck-Institut für Astronomie, the Max-Planck-Institut für Astrophysik, New Mexico State University, Princeton University, the US Naval Observatory, and the University of Washington. Apache Point Observatory, site of the SDSS telescopes, is operated by the Astrophysical Research Consortium. Funding for the project has been provided by the Alfred P. Sloan Foundation, the SDSS member institutions, the National Aeronautics and Space Administration, the National Science Foundation, the US Department of Energy, the Japanese Monbukagakusho,

²³ See http://home.fnal.gov/~dtucker/Southern_ugriz/index.html.

TABLE 8
THE $u'g'r'i'z'$ STANDARD-STAR NETWORK: CALIBRATED MAGNITUDES AND COLORS

Star Name	R.A. (J2000)	Decl. (J2000)	r'	$u' - g'$	$g' - r'$	$r' - i'$	$i' - z'$	$\sigma_{r'}$	$\sigma_{u' - g'}$	$\sigma_{g' - r'}$	$\sigma_{r' - i'}$	$\sigma_{i' - z'}$	$n_{u'}$	$n_{g'}$	$n_{r'}$	$n_{i'}$	$n_{z'}$
Hilt 31.....	00 28 11.15	+ 64 07 51.8	10.996	0.999	0.587	0.294	0.147	0.001	0.003	0.001	0.001	0.002	16	16	16	15	15
G158-100.....	00 33 54.60	-12 07 58.9	14.691	1.101	0.510	0.222	0.092	0.006	0.019	0.008	0.007	0.010	6	7	8	6	6
BD +71°0031.....	00 43 44.34	+ 72 10 43.1	10.091	0.896	0.260	0.079	0.007	0.001	0.003	0.002	0.002	0.004	14	14	14	14	14
SA 92-342.....	00 55 09.90	+ 00 43 12.9	11.527	1.069	0.257	0.049	-0.012	0.001	0.004	0.001	0.001	0.002	28	27	27	26	25
SA 92-263.....	00 55 39.41	+ 00 36 20.0	11.467	2.229	0.801	0.307	0.166	0.001	0.008	0.001	0.002	0.003	23	27	27	26	26
SA 92-502.....	00 56 08.13	+ 01 04 25.1	11.712	1.031	0.289	0.078	0.010	0.002	0.005	0.004	0.003	0.004	9	9	9	9	9
SA 92-282.....	00 56 46.86	+ 00 38 30.9	12.936	1.000	0.136	0.021	-0.009	0.004	0.017	0.004	0.006	0.016	5	6	5	5	3
SA 92-288.....	00 57 17.00	+ 00 36 48.7	11.350	1.768	0.661	0.233	0.098	0.002	0.013	0.005	0.003	0.005	6	6	6	5	5
SA 93-317.....	01 54 37.73	+ 00 43 00.5	11.437	1.068	0.317	0.084	0.002	0.001	0.008	0.003	0.002	0.004	16	16	16	16	16
SA 93-333.....	01 55 05.22	+ 00 45 42.5	11.760	1.742	0.633	0.203	0.089	0.002	0.006	0.004	0.003	0.004	16	16	16	15	16
SA 93-424.....	01 55 26.35	+ 00 56 42.5	11.300	2.410	0.823	0.281	0.123	0.002	0.025	0.003	0.003	0.016	10	9	9	8	9
Hilt 190.....	01 58 24.07	+ 61 53 43.5	10.883	0.903	0.640	0.318	0.224	0.002	0.004	0.003	0.003	0.003	17	17	17	17	17
LHS 14.....	02 12 20.99	+ 03 34 32.4	9.481	2.624	1.282	0.934	0.443	0.003	0.010	0.004	0.004	0.004	6	6	6	6	6
Hilt 233.....	02 12 29.97	+ 59 54 04.1	10.659	1.134	0.834	0.448	0.292	0.001	0.004	0.002	0.002	0.003	18	18	18	18	17
Feige 22.....	02 30 16.62	+ 05 15 50.6	13.024	0.050	-0.333	-0.303	-0.273	0.001	0.004	0.002	0.002	0.004	15	15	14	15	15
SA 94-242.....	02 57 21.24	+ 00 18 38.9	11.712	1.157	0.106	-0.033	-0.046	0.001	0.004	0.002	0.001	0.002	29	29	29	29	28
SA 94-251.....	02 57 46.98	+ 00 16 02.7	10.803	2.773	0.979	0.373	0.213	0.001	0.004	0.001	0.001	0.001	29	29	29	29	29
SA 94-702.....	02 58 13.37	+ 01 10 54.3	11.116	3.189	1.159	0.459	0.263	0.002	0.009	0.003	0.002	0.002	12	13	13	13	13
Ross 374.....	03 26 59.76	+ 23 46 35.9	10.646	1.027	0.385	0.141	0.050	0.002	0.004	0.003	0.003	0.003	12	12	12	12	12
Ross 34.....	03 28 53.14	+ 37 22 56.7	10.530	2.580	1.229	0.530	0.271	0.001	0.007	0.002	0.001	0.002	10	10	10	10	10
SA 95-96.....	03 52 54.18	+ 00 00 18.7	10.071	1.142	-0.070	-0.123	-0.051	0.002	0.004	0.003	0.002	0.001	11	11	10	11	11
SA 95-190.....	03 53 13.24	+ 00 16 22.8	12.593	1.300	0.126	0.002	0.043	0.002	0.004	0.003	0.003	0.004	9	9	9	9	9
SA 95-193.....	03 53 20.59	+ 00 16 34.7	13.844	2.489	1.097	0.407	0.214	0.004	0.017	0.006	0.005	0.006	3	8	9	9	9
Hilt 404.....	03 53 59.42	+ 53 12 56.8	10.815	1.034	0.656	0.342	0.250	0.002	0.004	0.003	0.003	0.004	17	17	17	17	16
SA 95-218.....	03 54 49.95	+ 00 10 08.5	11.901	1.442	0.500	0.167	0.058	0.001	0.007	0.002	0.003	0.006	6	6	6	6	6
SA 95-132.....	03 54 51.67	+ 00 05 21.5	11.994	1.481	0.252	0.078	0.053	0.003	0.007	0.005	0.004	0.005	6	6	6	6	6
SA 95-142.....	03 55 09.40	+ 00 01 20.6	12.775	1.272	0.422	0.163	0.088	0.005	0.011	0.006	0.007	0.009	5	5	5	5	5
SA 95-149.....	03 55 44.44	+ 00 07 02.8	10.375	3.181	1.326	0.625	0.371	0.004	0.013	0.006	0.006	0.007	8	11	13	11	13
SA 95-236.....	03 56 13.34	+ 00 08 47.0	11.287	1.414	0.539	0.196	0.084	0.003	0.007	0.004	0.005	0.006	13	13	13	12	13
BD +21°0607.....	04 14 35.51	+ 22 21 04.3	9.114	0.894	0.281	0.089	0.008	0.001	0.002	0.001	0.001	0.001	76	80	78	80	80
BD -21°0910.....	04 33 16.19	-21 08 07.1	9.608	1.364	0.474	0.143	0.036	0.002	0.006	0.003	0.003	0.004	14	14	12	14	14
SA 96-36.....	04 51 42.40	-00 10 09.4	10.614	1.196	0.027	-0.079	-0.072	0.002	0.004	0.003	0.003	0.003	16	16	16	16	16
SA 96-737.....	04 52 35.34	+ 00 22 30.2	11.275	2.770	1.099	0.492	0.271	0.003	0.009	0.004	0.004	0.004	13	12	13	13	14
SA 96-83.....	04 52 58.86	-00 14 41.3	11.793	1.237	-0.054	-0.110	-0.048	0.003	0.007	0.004	0.004	0.004	20	19	20	20	20
SA 96-235.....	04 53 18.87	-00 05 01.6	10.820	2.308	0.814	0.288	0.161	0.001	0.007	0.001	0.001	0.002	21	22	22	23	22
Ross 49.....	05 44 56.81	+ 09 14 32.2	11.163	1.130	0.467	0.162	0.049	0.001	0.004	0.002	0.001	0.002	16	16	15	16	16
SA 97-249.....	05 57 07.56	+ 00 01 11.6	11.567	1.317	0.451	0.141	0.038	0.001	0.005	0.002	0.001	0.002	19	19	19	19	19
SA 97-345.....	05 57 33.16	+ 00 21 16.4	11.005	3.397	1.424	0.640	0.426	0.002	0.010	0.004	0.003	0.003	10	18	20	20	20
SA 97-351.....	05 57 37.30	+ 00 13 44.0	9.813	1.130	0.008	-0.074	-0.022	0.002	0.004	0.004	0.003	0.003	19	19	19	20	20
SA 97-75.....	05 57 55.08	-00 09 28.5	10.783	3.878	1.618	0.756	0.491	0.002	0.017	0.004	0.003	0.004	9	14	14	14	13
SA 97-284.....	05 58 25.02	+ 00 05 13.5	10.299	2.641	1.155	0.521	0.320	0.002	0.008	0.002	0.003	0.004	10	10	11	10	10
SA 97-288.....	05 58 30.09	+ 00 06 40.7	10.718	1.331	0.401	0.106	0.013	0.002	0.003	0.002	0.003	0.004	10	10	11	10	10
Hilt 566.....	06 32 09.67	+ 03 34 44.4	10.787	1.125	0.673	0.341	0.211	0.002	0.004	0.003	0.003	0.003	30	29	30	29	30
LHS 1858.....	06 37 10.80	+ 17 33 53.3	9.007	2.763	1.374	0.736	0.365	0.002	0.004	0.003	0.003	0.003	15	15	16	15	15
SA 98-978.....	06 51 33.72	-00 11 31.5	10.414	1.277	0.407	0.106	0.013	0.001	0.005	0.002	0.002	0.004	21	20	21	21	23
SA 98-185.....	06 52 01.88	-00 27 21.6	10.610	1.153	-0.037	-0.093	-0.057	0.003	0.008	0.005	0.004	0.007	15	14	13	14	13
SA 98-193.....	06 52 03.37	-00 27 18.3	9.676	2.713	0.903	0.327	0.190	0.002	0.009	0.003	0.003	0.004	12	16	16	16	16

TABLE 8—Continued

Star Name	R.A. (J2000)	Decl. (J2000)	r'	$u' - g'$	$g' - r'$	$r' - i'$	$i' - z'$	$\sigma_{r'}$	$\sigma_{u' - g'}$	$\sigma_{g' - r'}$	$\sigma_{r' - i'}$	$\sigma_{i' - z'}$	$n_{u'}$	$n_{g'}$	$n_{r'}$	$n_{i'}$	$n_{z'}$
SA 98-653	06 52 04.94	-00 18 18.2	9.655	0.843	-0.212	-0.203	-0.114	0.002	0.005	0.003	0.002	0.002	23	22	24	24	24
SA 98-685	06 52 18.46	-00 20 19.5	11.857	1.218	0.287	0.070	-0.001	0.003	0.010	0.004	0.004	0.004	19	24	23	23	21
Ru 149F	07 24 14.02	-00 31 38.2	13.119	2.469	0.867	0.317	0.166	0.002	0.013	0.003	0.002	0.002	9	33	39	39	39
Ru 149D	07 24 15.36	-00 32 47.9	11.601	0.652	-0.213	-0.203	-0.136	0.001	0.003	0.001	0.001	0.001	40	40	40	40	40
Ru 149B	07 24 17.53	-00 33 05.4	12.474	1.385	0.460	0.141	0.033	0.001	0.006	0.002	0.001	0.002	36	40	40	40	39
LHS 33	07 27 24.49	+05 13 32.9	9.286	2.839	1.331	1.477	0.695	0.002	0.005	0.003	0.004	0.006	13	13	13	9	9
Ru 152	07 29 58.44	-02 06 37.5	13.188	-0.263	-0.355	-0.289	-0.252	0.002	0.005	0.004	0.005	0.007	9	9	9	9	5
SA 99-438	07 55 54.26	-00 16 49.1	9.569	0.136	-0.348	-0.293	-0.220	0.002	0.006	0.004	0.003	0.003	12	12	13	14	14
SA 99-447	07 56 06.68	-00 20 42.3	9.572	0.734	-0.287	-0.245	-0.161	0.003	0.005	0.004	0.004	0.003	13	13	14	16	16
BD +75°0325	08 10 49.50	+74 57 57.8	9.786	-0.508	-0.514	-0.382	-0.323	0.002	0.005	0.004	0.003	0.004	14	13	14	14	14
BD +8°2015	08 15 41.62	+07 37 05.9	10.194	1.393	0.497	0.173	0.065	0.002	0.005	0.003	0.002	0.003	21	20	21	20	21
BD +54°1216	08 19 22.56	+54 05 09.7	9.586	0.890	0.300	0.107	0.010	0.001	0.004	0.002	0.002	0.004	17	16	17	16	16
GCRV 5757	08 44 05.00	+36 14 43.9	10.803	1.000	0.403	0.152	0.048	0.001	0.004	0.002	0.002	0.003	13	13	13	13	13
BD +25°1981	08 44 24.68	+24 47 47.9	9.270	0.925	0.144	0.014	-0.037	0.002	0.004	0.003	0.003	0.004	19	19	19	18	19
SA 100-241	08 52 34.05	-00 39 48.8	10.204	1.165	-0.068	-0.128	-0.097	0.003	0.005	0.004	0.004	0.004	13	12	12	13	12
SA 100-280	08 53 35.47	-00 36 41.0	11.689	1.143	0.308	0.084	0.003	0.002	0.006	0.003	0.003	0.004	15	15	17	16	16
SA 100-394	08 53 54.51	-00 32 22.0	10.932	2.979	1.056	0.419	0.237	0.001	0.015	0.002	0.001	0.001	10	15	17	16	15
GCRV 5951	09 05 16.68	+38 47 54.7	11.474	0.854	0.346	0.135	0.029	0.002	0.004	0.004	0.003	0.004	11	11	11	11	11
PG 0918+029D ..	09 21 21.94	+02 47 28.7	11.937	2.227	0.817	0.324	0.166	0.002	0.010	0.003	0.003	0.004	17	18	18	18	19
BD +9°2190	09 29 15.55	+08 38 00.6	11.049	0.902	0.238	0.076	0.009	0.001	0.006	0.002	0.001	0.002	10	11	11	11	10
BD -12°2918	09 31 19.42	-13 29 19.3	9.476	2.817	1.326	1.201	0.561	0.002	0.005	0.003	0.004	0.004	11	11	12	10	11
Ross 889	09 40 43.19	+01 00 29.5	10.380	0.875	0.220	0.068	0.006	0.002	0.004	0.004	0.003	0.004	7	8	7	7	8
SA 101-315	09 54 51.28	-00 27 31.1	10.894	2.490	0.894	0.350	0.196	0.002	0.006	0.002	0.003	0.003	24	24	25	24	24
SA 101-316	09 54 52.03	-00 18 34.4	11.438	1.152	0.309	0.073	0.007	0.001	0.005	0.001	0.001	0.003	24	24	24	24	24
SA 101-207	09 57 52.48	-00 47 36.4	12.290	1.085	0.347	0.101	0.022	0.002	0.005	0.003	0.004	0.004	11	11	10	11	11
G162-66	10 33 42.81	-11 41 38.7	13.227	-0.183	-0.387	-0.354	-0.303	0.001	0.014	0.005	0.007	0.014	4	4	3	4	4
Feige 34	10 39 36.73	+43 06 09.2	11.423	-0.509	-0.508	-0.347	-0.265	0.002	0.004	0.003	0.002	0.003	16	16	16	16	16
BD +29°2091	10 47 23.16	+28 23 56.0	10.123	0.864	0.366	0.132	0.040	0.006	0.012	0.008	0.008	0.006	9	9	8	8	9
PG 1047+003A ..	10 50 05.65	-00 01 11.3	13.303	1.385	0.519	0.212	0.087	0.003	0.009	0.004	0.004	0.005	15	20	21	20	20
Ross 106	10 50 28.98	+56 26 31.0	12.413	1.028	0.434	0.176	0.060	0.003	0.008	0.004	0.004	0.006	10	10	9	10	10
SA 102-620	10 55 04.22	-00 48 18.9	9.665	2.464	0.932	0.309	0.148	0.002	0.009	0.003	0.003	0.004	11	11	9	11	11
G163-50	11 07 59.97	-05 09 26.0	13.266	0.215	-0.277	-0.272	-0.271	0.003	0.004	0.004	0.004	0.007	16	16	16	16	14
G163-51	11 08 06.55	-05 13 46.9	11.960	2.741	1.315	1.238	0.567	0.003	0.014	0.004	0.004	0.004	8	17	17	12	12
Wolf 365	11 11 00.00	+06 25 11.3	11.135	1.182	0.560	0.237	0.097	0.003	0.007	0.004	0.004	0.005	12	12	11	13	13
GCRV 7017	11 32 23.31	+76 39 18.1	11.326	1.120	0.517	0.212	0.080	0.003	0.006	0.005	0.004	0.005	12	12	12	12	12
BD -21°3420	11 55 28.45	-22 23 13.3	10.021	0.998	0.322	0.122	0.036	0.008	0.010	0.009	0.012	0.011	8	6	5	8	8
SA 103-626	11 56 46.14	-00 23 14.6	11.753	1.056	0.246	0.056	-0.027	0.003	0.009	0.004	0.004	0.006	15	15	14	16	13
SA 103-526	11 56 54.18	-00 30 13.5	10.575	2.434	0.826	0.293	0.164	0.002	0.011	0.004	0.003	0.004	10	17	14	16	16
Ross 453	12 10 55.77	+00 23 54.3	10.971	0.872	0.298	0.101	0.025	0.005	0.009	0.006	0.006	0.006	12	10	11	13	13
Feige 66	12 37 23.52	+25 03 59.9	10.747	-0.345	-0.476	-0.367	-0.316	0.002	0.003	0.002	0.002	0.004	15	16	17	17	16
SA 104-428	12 41 41.31	-00 26 26.5	12.330	2.153	0.763	0.279	0.147	0.002	0.008	0.004	0.004	0.005	7	11	12	12	11
SA 104-598	12 45 16.78	-00 16 40.4	11.057	2.481	0.985	0.339	0.148	0.005	0.015	0.006	0.006	0.006	8	9	9	11	10
Ross 484	13 18 56.71	-03 04 18.0	10.378	2.000	0.855	0.327	0.165	0.003	0.009	0.004	0.004	0.006	8	9	9	9	9
LTT 5137	13 20 23.67	-03 01 41.8	11.190	1.103	0.455	0.181	0.063	0.004	0.011	0.006	0.005	0.007	7	6	6	6	7
GCRV 7951	13 21 47.60	+74 12 32.9	11.488	0.876	0.341	0.134	0.035	0.001	0.005	0.002	0.001	0.003	11	12	12	12	12
PG 1323-086D ..	13 26 05.26	-08 50 35.7	11.928	1.210	0.397	0.132	0.032	0.001	0.003	0.001	0.001	0.002	22	21	23	23	22
G14-55	13 28 21.09	-02 21 36.7	10.633	2.813	1.325	1.333	0.615	0.002	0.007	0.004	0.003	0.004	13	13	13	12	13
BD +30°2428B ..	13 37 13.80	+30 05 14.2	10.239	1.844	0.668	0.223	0.107	0.003	0.006	0.004	0.004	0.004	10	10	10	10	10

TABLE 8—Continued

Star Name	R.A. (J2000)	Decl. (J2000)	r'	$u' - g'$	$g' - r'$	$r' - i'$	$i' - z'$	$\sigma_{r'}$	$\sigma_{u' - g'}$	$\sigma_{g' - r'}$	$\sigma_{r' - i'}$	$\sigma_{i' - z'}$	$n_{u'}$	$n_{g'}$	$n_{r'}$	$n_{i'}$	$n_{z'}$
SA 105-815.....	13 40 02.50	-00 02 18.8	11.366	0.863	0.232	0.076	0.003	0.002	0.005	0.003	0.004	0.005	13	13	13	13	13
BD + 2°2711.....	13 42 19.01	+01 30 18.6	10.548	0.166	-0.362	-0.301	-0.234	0.002	0.005	0.004	0.004	0.005	10	10	10	10	10
HD 121968.....	13 58 51.17	-02 54 52.3	10.425	-0.064	-0.370	-0.318	-0.245	0.003	0.005	0.004	0.005	0.005	5	6	6	6	5
Ross 838	14 01 44.47	+08 55 17.4	11.327	1.277	0.573	0.239	0.111	0.002	0.007	0.003	0.003	0.004	17	17	17	16	16
BD + 26°2606.....	14 49 02.35	+25 42 09.2	9.604	0.870	0.287	0.101	0.017	0.001	0.001	0.001	0.001	0.001	122	125	124	126	125
GCRV 8758	15 07 41.38	+32 24 37.2	10.954	1.258	0.492	0.176	0.062	0.002	0.004	0.003	0.003	0.004	15	15	15	15	15
PG 1528 + 062B ..	15 30 39.55	+06 01 13.1	11.828	1.235	0.419	0.143	0.036	0.001	0.004	0.001	0.001	0.002	32	33	33	33	33
G15-24.....	15 30 41.76	+08 23 40.4	11.277	1.035	0.412	0.151	0.052	0.002	0.004	0.003	0.003	0.004	11	11	11	11	11
SA 107-1006.....	15 38 33.37	+00 14 19.2	11.474	1.549	0.578	0.204	0.090	0.002	0.007	0.003	0.003	0.003	15	16	16	16	16
SA 107-351.....	15 38 45.75	-00 32 06.5	12.175	1.187	0.396	0.142	0.048	0.002	0.004	0.003	0.003	0.004	14	15	15	15	15
BD + 33°2642.....	15 51 59.88	+32 56 54.3	10.979	-0.018	-0.332	-0.284	-0.212	0.001	0.003	0.002	0.002	0.004	23	25	25	26	25
Ross 530	16 19 51.66	+22 38 20.2	11.319	1.273	0.558	0.229	0.103	0.002	0.004	0.003	0.002	0.002	28	28	28	28	27
GCRV 9483	16 28 16.87	+44 40 38.3	11.104	1.106	0.527	0.222	0.082	0.002	0.004	0.003	0.003	0.004	17	17	17	17	17
SA 108-475.....	16 37 00.60	-00 34 39.0	10.832	3.127	1.130	0.456	0.270	0.002	0.015	0.003	0.002	0.003	8	17	17	17	17
SA 108-551.....	16 37 47.79	-00 33 05.1	10.747	1.256	-0.032	-0.104	-0.051	0.002	0.006	0.004	0.003	0.004	16	16	16	16	16
Wolf 629	16 55 25.66	-08 19 13.1	11.129	3.013	1.413	1.466	0.648	0.001	0.021	0.004	0.004	0.004	4	4	4	4	4
BD + 18°3407.....	17 35 19.89	+18 53 00.8	9.765	1.690	0.628	0.227	0.100	0.001	0.003	0.001	0.001	0.001	37	37	37	37	37
BD + 2°3375.....	17 39 45.59	+02 24 59.6	9.809	0.886	0.321	0.123	0.029	0.001	0.002	0.001	0.001	0.002	41	42	43	41	42
SA 109-71	17 44 06.78	-00 24 57.8	11.475	1.274	0.130	0.010	0.010	0.001	0.004	0.002	0.001	0.002	25	25	25	25	25
SA 109-381.....	17 44 12.26	-00 20 32.7	11.514	1.477	0.547	0.223	0.094	0.002	0.006	0.003	0.002	0.002	25	25	25	25	25
SA 109-231.....	17 45 19.95	-00 25 51.6	8.825	3.231	1.218	0.502	0.314	0.003	0.016	0.004	0.004	0.003	8	12	12	12	12
SA 109-537.....	17 45 42.45	-00 21 35.4	10.201	1.449	0.456	0.191	0.079	0.003	0.008	0.004	0.004	0.005	10	9	10	11	12
Hilt 733	18 17 23.32	-11 44 57.5	10.939	1.102	0.827	0.410	0.260	0.002	0.008	0.004	0.003	0.004	5	5	13	13	10
Ross 711	18 35 19.17	+28 41 55.3	11.295	0.837	0.282	0.104	0.015	0.001	0.005	0.002	0.002	0.004	20	19	19	19	20
SA 110-232.....	18 40 52.33	+00 01 54.8	12.287	1.390	0.552	0.237	0.094	0.001	0.005	0.002	0.002	0.004	16	16	16	16	16
SA 110-340.....	18 41 28.44	+00 15 23.0	10.010	1.228	0.094	-0.039	-0.053	0.003	0.005	0.004	0.004	0.003	13	13	13	13	11
SA 110-499.....	18 43 07.66	+00 28 01.4	11.399	2.036	0.827	0.473	0.332	0.002	0.007	0.003	0.003	0.004	18	17	18	17	17
SA 110-503.....	18 43 11.69	+00 29 42.9	11.625	1.792	0.460	0.222	0.116	0.002	0.005	0.003	0.004	0.004	18	17	18	17	17
GJ 745A.....	19 07 05.57	+20 53 16.9	10.159	2.848	1.408	1.046	0.490	0.001	0.004	0.002	0.002	0.004	15	15	16	15	15
GJ 745B.....	19 07 13.19	+20 52 37.2	10.151	2.839	1.401	1.049	0.488	0.001	0.006	0.002	0.002	0.003	17	17	17	17	17
BD + 35°3659.....	19 31 09.22	+36 09 10.1	10.089	0.925	0.333	0.117	0.022	0.001	0.002	0.001	0.001	0.001	34	34	34	32	32
SA 111-775.....	19 37 16.36	+00 12 05.5	10.106	3.765	1.491	0.697	0.421	0.003	0.019	0.005	0.004	0.004	7	11	11	11	11
SA 111-1925.....	19 37 28.62	+00 25 03.1	12.345	1.397	0.200	0.061	0.051	0.002	0.011	0.004	0.005	0.007	11	14	14	10	12
Wolf 1346	20 34 21.89	+25 03 49.7	11.753	-0.016	-0.351	-0.309	-0.291	0.001	0.002	0.001	0.001	0.002	22	22	22	22	21
SA 112-223.....	20 42 14.58	+00 08 59.7	11.336	1.145	0.270	0.062	0.000	0.002	0.006	0.004	0.003	0.004	23	23	23	22	22
SA 112-250.....	20 42 26.38	+00 07 42.4	11.962	1.162	0.352	0.116	0.008	0.002	0.008	0.004	0.003	0.004	23	23	22	23	21
SA 112-805.....	20 42 46.74	+00 16 08.4	12.174	1.183	-0.087	-0.135	-0.090	0.003	0.005	0.004	0.004	0.009	8	8	8	8	7
SA 112-822.....	20 42 54.90	+00 15 01.9	11.227	2.293	0.801	0.288	0.154	0.003	0.021	0.004	0.004	0.004	7	8	8	8	8
BD + 62°1916.....	21 15 05.74	+62 50 27.9	9.332	1.568	0.540	0.171	0.061	0.001	0.004	0.002	0.001	0.002	15	15	15	15	15
SA 113-339.....	21 40 55.64	+00 27 58.2	12.103	1.149	0.389	0.127	0.035	0.001	0.004	0.002	0.001	0.003	15	15	15	15	15
SA 113-466.....	21 41 27.39	+00 40 15.6	9.908	1.125	0.275	0.073	-0.005	0.002	0.003	0.002	0.002	0.002	24	24	24	24	24
SA 113-259.....	21 41 44.84	+00 17 39.9	11.376	2.705	0.933	0.336	0.193	0.002	0.011	0.003	0.003	0.004	10	14	14	14	14
SA 113-260.....	21 41 48.03	+00 23 53.3	12.284	1.217	0.331	0.080	0.015	0.002	0.006	0.003	0.003	0.005	14	14	14	14	14
SA 113-475.....	21 41 51.30	+00 39 20.8	9.979	2.255	0.817	0.318	0.166	0.001	0.008	0.001	0.001	0.002	24	24	24	24	24
BD + 28°4211.....	21 51 11.02	+28 51 50.4	10.750	-0.517	-0.511	-0.379	-0.313	0.003	0.004	0.004	0.004	0.003	16	16	16	16	16
G93-48.....	21 52 25.37	+02 23 19.6	12.961	0.107	-0.308	-0.307	-0.261	0.004	0.006	0.006	0.004	0.012	6	6	6	6	4
BD + 25°4655.....	21 59 41.96	+26 25 57.3	9.929	-0.427	-0.479	-0.375	-0.328	0.002	0.004	0.003	0.003	0.004	12	12	12	12	12
Hilt 1089	22 09 20.87	+57 51 28.4	10.639	1.512	0.552	0.189	0.073	0.001	0.004	0.001	0.001	0.002	14	14	16	16	14

TABLE 8—Continued

Star Name	R.A. (J2000)	Decl. (J2000)	r'	$u' - g'$	$g' - r'$	$r' - i'$	$i' - z'$	$\sigma_{r'}$	$\sigma_{u' - g'}$	$\sigma_{g' - r'}$	$\sigma_{r' - i'}$	$\sigma_{i' - z'}$	$n_{u'}$	$n_{g'}$	$n_{r'}$	$n_{i'}$	$n_{z'}$
BD +17°4708.....	22 11 31.37	+ 18 05 34.1	9.350	0.920	0.290	0.100	0.020	0.001	0.001	0.001	0.001	0.001	114	114	115	114	114
BD -11°5781.....	22 13 10.68	-11 10 38.4	9.178	1.966	0.720	0.236	0.130	0.004	0.009	0.006	0.005	0.005	15	12	11	12	15
SA 114-531.....	22 40 36.78	+ 00 51 55.6	11.880	1.419	0.540	0.187	0.080	0.002	0.010	0.003	0.003	0.004	10	11	11	11	11
SA 114-654.....	22 41 26.14	+ 01 10 10.7	11.672	1.398	0.449	0.137	0.040	0.001	0.004	0.001	0.001	0.002	20	20	20	19	19
SA 114-656.....	22 41 35.06	+ 01 11 09.8	12.326	1.961	0.756	0.293	0.156	0.001	0.008	0.002	0.002	0.004	18	20	20	20	20
SA 114-548.....	22 41 36.83	+ 00 59 05.7	11.135	3.146	1.120	0.442	0.252	0.003	0.009	0.004	0.003	0.003	12	12	13	13	13
SA 114-750.....	22 41 44.70	+ 01 12 36.2	12.021	0.548	-0.212	-0.230	-0.163	0.002	0.005	0.003	0.003	0.004	20	20	20	19	19
G27-45.....	22 44 56.30	-02 21 12.8	11.282	1.111	0.503	0.193	0.081	0.002	0.004	0.003	0.003	0.003	11	11	11	11	11
Ross 786	23 09 33.34	+ 00 43 02.1	9.706	1.221	0.540	0.224	0.093	0.003	0.006	0.005	0.004	0.004	13	13	14	14	14
GD 246	23 12 23.07	+ 10 47 04.2	13.346	-0.491	-0.504	-0.378	-0.367	0.001	0.004	0.002	0.003	0.006	11	10	11	11	10
BD +38°4955.....	23 13 38.81	+ 39 25 02.6	10.800	1.038	0.515	0.220	0.096	0.001	0.005	0.001	0.001	0.002	13	12	13	13	13
BD +33°4737.....	23 34 36.13	+ 34 02 22.2	8.840	1.653	0.572	0.177	0.062	0.002	0.004	0.003	0.003	0.003	16	16	16	16	16
PG 2336+004B ...	23 38 38.26	+ 00 42 46.4	12.312	1.101	0.336	0.100	0.014	0.001	0.007	0.003	0.002	0.005	14	14	14	14	14
SA 115-420.....	23 42 36.48	+ 01 05 58.8	11.063	1.091	0.290	0.080	0.007	0.002	0.004	0.003	0.002	0.003	18	19	19	19	18
SA 115-516.....	23 44 15.38	+ 01 14 12.5	10.107	2.167	0.807	0.317	0.172	0.002	0.009	0.004	0.003	0.004	16	16	16	16	16

TABLE 9
THE $u'g'r'i'z'$ STANDARD-STAR NETWORK: ASTROMETRY, SPECTRAL PROPERTIES, AND NOTES

Star Name (1)	α (J2000) (2)	δ (J2000) (3)	Other ID (4)	Epoch (yr) (5)	$\mu(\alpha \cos \delta)$ (mas yr $^{-1}$) (6)	$\sigma(\mu(\alpha \cos \delta))$ (mas yr $^{-1}$) (7)	$\mu(\delta)$ (mas yr $^{-1}$) (8)	$\sigma(\mu(\delta))$ (mas yr $^{-1}$) (9)	PM Ref. (10)	Spectral Type (11)	Spectrum Ref. (12)	Notes (13)
Hilt 31	00 28 11.15	+ 64 07 51.8	Tycho	2000.000	-3.90	3.40	-4.90	3.50	TYC2	B1 V	H56	1
G158-100	00 33 54.60	-12 07 58.9	GSC 05271-00531	2000.000	152.00	3.00	-179.00	4.00	HD80	DG	G84	w, 2
BD +71°0031	00 43 44.34	+ 72 10 43.1	HIP 3430	2000.000	321.50	1.80	90.70	1.80	TYC2	sdF5	C83	m
SA 92-342	00 55 09.90	+ 00 43 12.9	Tycho	2000.000	-2.20	1.70	-0.20	1.70	TYC2	F5	DL79	
SA 92-263	00 55 39.41	+ 00 36 20.0	GSC 00012-00675	1983.702		G8 III	DL79	
SA 92-502	00 56 08.13	+ 01 04 25.1	Tycho	2000.000	7.20	1.70	7.40	1.70	TYC2		...	
SA 92-282	00 56 46.86	+ 00 38 30.9	Tycho	2000.000	28.30	2.80	6.10	2.70	TYC2	A5	DL79	
SA 92-288	00 57 17.00	+ 00 36 48.7	Tycho	2000.000	4.90	1.40	4.90	1.40	TYC2	K3 V	DL79	
SA 93-317	01 54 37.73	+ 00 43 00.5	Tycho	2000.000	-9.30	1.60	-18.50	1.70	TYC2	F5	DL79	
SA 93-333	01 55 05.22	+ 00 45 42.5	Tycho	2000.000	18.60	1.70	-1.80	2.00	TYC2	G5	DL79	
SA 93-424	01 55 26.35	+ 00 56 42.5	Tycho	2000.000	3.70	1.70	-3.40	1.90	TYC2	G8 III	DL79	
Hilt 190	01 58 24.07	+ 61 53 43.5	Tycho	2000.000	-6.40	2.90	-1.60	2.90	TYC2	B1 V:	H56	
LHS 14	02 12 20.99	+ 03 34 32.4	HIP 10279	2000.000	-1761.70	1.60	-1851.70	1.60	TYC2	M1.5	MSU	m
Hilt 233	02 12 29.97	+ 59 54 04.1	Tycho	2000.000	3.30	3.60	-3.80	3.70	TYC2	O9 V	H56	3
Feige 22	02 30 16.62	+ 05 15 50.6	HIP 11650	2000.000	71.15	6.60	-24.60	4.20	HIP	DA3	GE87	4
SA 94-242	02 57 21.24	+ 00 18 38.9	GSC 00048-01015	1983.703		A2	MSU	
SA 94-251	02 57 46.98	+ 00 16 02.7	GSC 00048-01221	1983.703		K1 III	DL79	
SA 94-702	02 58 13.37	+ 01 10 54.3	GSC 00048-00918	1983.703		K2:	DL79	
Ross 374	03 26 59.76	+ 23 46 35.9	HIP 16072	2000.000	262.70	1.50	-348.60	1.50	HIP	F5	B85	m
Ross 34	03 28 53.14	+ 37 22 56.7	HIP 16209	2000.000	1120.24	2.70	-1065.81	2.70	HIP	sdK7	G97	m
SA 95-96	03 52 54.18	+ 00 00 18.7	Tycho	2000.000	13.80	0.90	-1.60	0.90	TYC2	A0	DL79	
SA 95-190	03 53 13.24	+ 00 16 22.8	Tycho	2000.000	-1.90	1.90	-1.00	2.00	TYC2			
SA 95-193	03 53 20.59	+ 00 16 34.7	GSC 00066-00670	1984.729				
Hilt 404	03 53 59.42	+ 53 12 56.8	Tycho	2000.000	-3.40	2.20	1.20	2.10	TYC2	B1 V	H56	
SA 95-218	03 54 49.95	+ 00 10 08.5	GSC 00066-00856	1984.729		G2 V	DL79	
SA 95-132	03 54 51.67	+ 00 05 21.5	Tycho	2000.000	-4.90	2.30	-9.90	2.40	TYC2	A4	DL79	
SA 95-142	03 55 09.40	+ 00 01 20.6	GSC 00066-00917	1984.729				
SA 95-149	03 55 44.44	+ 00 07 02.8	Tycho	2000.000	21.30	2.10	-19.80	2.10	TYC2	G9 IV	DL79	
SA 95-236	03 56 13.34	+ 00 08 47.0	Tycho	2000.000	15.60	2.20	40.70	2.20	TYC2	G5 IV	DL79	
BD +21°0607	04 14 35.51	+ 22 21 04.3	HIP 19797	2000.000	427.30	0.90	-303.40	0.90	TYC2	sdF5	C83	m
BD -21°0910	04 33 16.19	-21 08 07.1	HIP 21232	2000.000	-32.20	1.60	-185.90	1.60	TYC2	G5 V	MSS88	m
SA 96-36	04 51 42.40	-00 10 09.4	Tycho	2000.000	-13.90	1.20	-1.80	1.20	TYC2	A2	DL79	
SA 96-737	04 52 35.34	+ 00 22 30.2	GSC 00085-00158	1983.774		K0	SIMBAD	5
SA 96-83	04 52 58.86	-00 14 41.3	Tycho	2000.000	0.30	1.30	-3.20	1.30	TYC2	A3	DL79	
SA 96-235	04 53 18.87	-00 05 01.6	Tycho	2000.000	3.00	1.50	0.70	1.50	TYC2	G9 III	DL79	
Ross 49	05 44 56.81	+ 09 14 32.2	HIP 27111	2000.000	86.80	2.50	-634.80	2.50	TYC2	F8:	B85	6
SA 97-249	05 57 07.56	+ 00 01 11.6	Tycho	2000.000	19.30	1.70	2.40	1.70	TYC2	G5 V	DL79	
SA 97-345	05 57 33.16	+ 00 21 16.4	GSC 00117-00815	1983.848		G8 III:	DL79	
SA 97-351	05 57 37.30	+ 00 13 44.0	Tycho	2000.000	1.30	1.20	-0.80	1.10	TYC2	A0	DL79	
SA 97-75	05 57 55.08	-00 09 28.5	Tycho	1991.850		K5:	DL79	
SA 97-284	05 58 25.02	+ 00 05 13.5	Tycho	2000.000	0.30	1.50	-4.40	1.50	TYC2	G8 III	DL79	7
SA 97-288	05 58 30.09	+ 00 06 40.7	Tycho	2000.000	0.40	1.90	-15.20	1.90	TYC2	G0	DL79	
Hilt 566	06 32 09.67	+ 03 34 44.4	Tycho	2000.000	4.00	1.70	0.90	1.80	TYC2	F5	HD	8
LHS 1858	06 37 10.80	+ 17 33 53.3	HIP 31635	2000.000	-765.40	1.60	338.10	1.50	TYC2	dM1	W94	m, 9
SA 98-978	06 51 33.72	-00 11 31.5	Tycho	2000.000	25.20	1.30	-29.60	1.30	TYC2	G3 V	DL79	
SA 98-185	06 52 01.88	-00 27 21.6	Tycho	2000.000	1.00	1.20	0.10	1.20	TYC2	A2	DL79	

TABLE 9—Continued

Star Name (1)	α (J2000) (2)	δ (J2000) (3)	Other ID (4)	Epoch (yr) (5)	$\mu(\alpha \cos \delta)$ (mas yr $^{-1}$) (6)	$\sigma(\mu(\alpha \cos \delta))$ (mas yr $^{-1}$) (7)	$\mu(\delta)$ (mas yr $^{-1}$) (8)	$\sigma(\mu(\delta))$ (mas yr $^{-1}$) (9)	PM Ref. (10)	Spectral Type (11)	Spectrum Ref. (12)	Notes (13)
SA 98-193	06 52 03.37	-00 27 18.3	Tycho	2000.000	2.80	1.20	-10.90	1.20	TYC2	K1 III	DL79	
SA 98-653	06 52 04.94	-00 18 18.2	Tycho	2000.000	-0.30	1.10	-3.50	1.10	TYC2	B9	DL79	
SA 98-685	06 52 18.46	-00 20 19.5	Tycho	2000.000	-0.60	2.50	-2.80	2.70	TYC2	F8	DL79	
Ru 149F	07 24 14.02	-00 31 38.2	GSC 04817-00748	1982.895	
Ru 149D	07 24 15.36	-00 32 47.9	Tycho	2000.000	-2.40	1.50	-1.80	1.50	TYC2		...	
Ru 149B	07 24 17.53	-00 33 05.4	GSC 04817-00990	1982.895	
LHS 33	07 27 24.49	+05 13 32.9	HIP 36208	2000.000	573.60	2.40	-3691.00	2.30	TYC2	M3.5 V	HK94	m, 10
Ru 152	07 29 58.44	-02 06 37.5	GSC 04821-00403	1982.895		O5 V	T90	p
SA 99-438	07 55 54.26	-00 16 49.1	Tycho	2000.000	-19.20	0.90	17.20	1.00	TYC2	B2	DL79	11
SA 99-447	07 56 06.68	-00 20 42.3	Tycho	2000.000	-9.90	1.00	-4.50	1.00	TYC2	B8	DL79	12
BD +75°0325	08 10 49.50	+74 57 57.8	HIP 40047	2000.000	9.10	1.10	10.60	1.20	TYC2	sdOp	BH80	
BD +8°2015	08 15 41.62	+07 37 05.9	Tycho	2000.000	-223.00	4.60	-157.00	4.50	TYC1	A2	SAO	13
BD +54°1216	08 19 22.56	+54 05 09.7	HIP 40778	2000.000	-35.80	1.30	-625.90	1.40	TYC2	sdF6	CH67	m
GCRV 5757	08 44 05.00	+36 14 43.9	HIP 42864	2000.000	-22.40	3.60	-457.70	3.30	TYC2	sdF8	P43	14
BD +25°1981	08 44 24.68	+24 47 47.9	HIP 42887	2000.000	-112.60	1.30	-348.40	1.20	TYC2	sdF2	S69	
SA 100-241	08 52 34.05	-00 39 48.8	Tycho	2000.000	1.00	1.20	-2.10	1.10	TYC2	A3	DL79	
SA 100-280	08 53 35.47	-00 36 41.0	Tycho	2000.000	11.20	2.10	-8.40	2.10	TYC2	F8	DL79	
SA 100-394	08 53 54.51	-00 32 22.0	Tycho	2000.000	-2.80	2.00	2.00	2.00	TYC2	K2 III:	DL79	
GCRV 5951	09 05 16.68	+38 47 54.7	HIP 44605	2000.000	4.60	2.30	-471.20	2.20	TYC2	sdF5	P43	m
PG 0918+029D	09 21 21.94	+02 47 28.7	Tycho	1982.878	
BD +9°2190	09 29 15.55	+08 38 00.6	HIP 46516	2000.000	199.00	1.80	-307.80	1.70	TYC2	sdA5	ES59	
BD -12°2918	09 31 19.42	-13 29 19.3	HIP 46706	2000.000	730.30	1.60	23.10	1.60	TYC2	M3	MSU	15
Ross 889	09 40 43.19	+01 00 29.5	Tycho	2000.000	148.20	1.50	-508.60	1.50	TYC2	sdA4	P43	16
SA 101-315	09 54 51.28	-00 27 31.1	Tycho	2000.000	-3.70	1.80	-1.50	1.90	TYC2	K0 III	DL79	
SA 101-316	09 54 52.03	-00 18 34.4	Tycho	2000.000	2.80	1.80	-10.60	1.80	TYC2	F6	DL79	
SA 101-207	09 57 52.48	-00 47 36.4	Tycho	2000.000	-4.30	2.00	4.20	2.00	TYC2	F8	DL79	
G162-66	10 33 42.81	-11 41 38.7	GSC 05495-00166	2000.000	-297.00	30.00	-55.00	30.00	G78	DA2	HBS98	w, 17
Feige 34	10 39 36.73	+43 06 09.2	HIP 52181	2000.000	12.00	1.50	-24.90	1.50	TYC2	D0	S96	s, 18
BD +29°2091	10 47 23.16	+28 23 56.0	HIP 52771	2000.000	179.40	1.40	-824.50	1.40	TYC2	sdG5	C83	m
PG 1047+003A	10 50 05.65	-00 01 11.3	GSC 04914-00008	1982.368	
Ross 106	10 50 28.98	+56 26 31.0	GSC 03826-00684	2000.000	158.00	5.00	-401.00	4.00	NLTT	G8:	NLTT	m
SA 102-620	10 55 04.22	-00 48 18.9	HIP 53383	2000.000	-235.20	1.20	13.40	1.20	TYC2	M0 III	DL79	
G163-50	11 07 59.97	-05 09 26.0	GSC 04927-00597	2000.000	-38.00	30.00	-426.00	30.00	G78	DA3	GE87	m, w, 19
G163-51	11 08 06.55	-05 13 46.9	GSC 04927-01272	2000.000	-38.00	30.00	-426.00	30.00	G78	M3	MSU	m, 20
Wolf 365	11 11 00.00	+06 25 11.3	HIP 54639	2000.000	-568.50	2.20	-517.70	2.10	TYC2	sdG3	P42	m
GCRV 7017	11 32 23.31	+76 39 18.1	HIP 56291	2000.000	115.20	2.00	-599.70	2.20	TYC2	sdG0	P42	m
BD -21°3420	11 55 28.45	-22 23 13.3	HIP 58145	2000.000	-156.40	1.70	-199.80	2.10	TYC2	F5 V	SAO	
SA 103-626	11 56 46.14	-00 23 14.6	Tycho	2000.000	15.40	2.40	-6.20	2.50	TYC2	F3	DL79	
SA 103-526	11 56 54.18	-00 30 13.5	Tycho	2000.000	-13.00	1.20	13.90	1.20	TYC2	K0 III	DL79	21
Ross 453	12 10 55.77	+00 23 54.3	HIP 59376	2000.000	-56.10	1.30	-436.40	1.30	TYC2	sdF2	P43	m
Feige 66	12 37 23.52	+25 03 59.9	HIP 61602	2000.000	2.60	1.40	-27.40	1.40	TYC2	sdOB	E96	
SA 104-428	12 41 41.31	-00 26 26.5	GSC 04949-00310	1987.330	
SA 104-598	12 45 16.78	-00 16 40.4	Tycho	2000.000	-138.30	1.40	-76.90	1.50	TYC2	K5 V	DL79	
Ross 484	13 18 56.71	-03 04 18.0	HIP 64965	2000.000	-643.00	4.10	-130.20	4.40	TYC2	dK8.5	DB90	m, 22
LTT 5137	13 20 23.67	-03 01 41.8	HIP 65081	2000.000	29.70	1.80	-191.80	1.80	TYC2		m	
GCRV 7951	13 21 47.60	+74 12 32.9	HIP 65206	2000.000	-443.90	2.00	40.00	2.10	TYC2	sdF2	YTP95	m
PG 1323-086D	13 26 05.26	-08 50 35.7	GSC 05544-00406	1983.194	

TABLE 9—Continued

Star Name (1)	α (J2000) (2)	δ (J2000) (3)	Other ID (4)	Epoch (yr) (5)	$\mu(\alpha \cos \delta)$ (mas yr $^{-1}$) (6)	$\sigma(\mu(\alpha \cos \delta))$ (mas yr $^{-1}$) (7)	$\mu(\delta)$ (mas yr $^{-1}$) (8)	$\sigma(\mu(\delta))$ (mas yr $^{-1}$) (9)	PM Ref. (10)	Spectral Type (11)	Spectrum Ref. (12)	Notes (13)
G14-55.....	13 28 21.09	-02 21 36.7	HIP 65714	2000.000	153.00	1.70	-491.80	1.80	TYC2	M3	MSU	23
BD +30°2428B....	13 37 13.80	+ 30 05 14.2	HIP 66441	2000.000	-158.30	2.40	41.10	2.30	TYC2	K1	MSU	24
SA 105-815.....	13 40 02.50	-00 02 18.8	HIP 66673	2000.000	-226.80	1.50	-83.30	1.50	TYC2	A0	DL79	m, 25
BD +2°2711.....	13 42 19.01	+ 01 30 18.6	HIP 66872	2000.000	-6.10	1.20	0.50	1.20	TYC2	B4 V	LD95	m
HD 121968.....	13 58 51.17	-02 54 52.3	HIP 68297	2000.000	1.60	1.10	18.20	1.20	TYC2	B2 II	MSS99	
Ross 838	14 01 44.47	+ 08 55 17.4	HIP 68527	2000.000	157.40	2.60	-748.20	2.50	TYC2	sdG3	P43	m
BD +26°2606.....	14 49 02.35	+ 25 42 09.2	HIP 72461	2000.000	-8.50	1.30	-345.50	1.20	TYC2	sdF4	C83	m
GCRV 8758	15 07 41.38	+ 32 24 37.2	74029	2000.000	-136.00	1.90	-458.70	1.80	TYC2	G6 V	CH67	
PG 1528+062B	15 30 39.55	+ 06 01 13.1	Tycho	2000.000	-12.70	2.60	7.20	2.50	TYC2	...		
G15-24.....	15 30 41.76	+ 08 23 40.4	HIP 75946	2000.000	-394.70	2.60	-118.40	2.50	TYC2	G4	J66	
SA 107-1006.....	15 38 33.37	+ 00 14 19.2	Tycho	2000.000	25.80	2.50	-22.80	2.50	TYC2	G5 V	DL79	
SA 107-351.....	15 38 45.75	-00 32 06.5	Tycho	2000.000	-12.60	2.20	-7.40	2.20	TYC2	F8	DL79	
BD +33°2642.....	15 51 59.88	+ 32 56 54.3	HIP 77716	2000.000	-10.10	1.80	3.70	1.90	TYC2	B2 IVp	Ir58	p
Ross 530	16 19 51.66	+ 22 38 20.2	HIP 80003	2000.000	-40.27	1.98	-451.15	2.32	HIP	sdG2:	P43	m
GCRV 9483	16 28 16.87	+ 44 40 38.3	HIP 80679	2000.000	-266.90	1.50	-687.20	1.40	TYC2	G5	B85	m
SA 108-475.....	16 37 00.60	-00 34 39.0	Tycho	2000.000	-0.30	2.00	-0.60	2.10	TYC2	K0 III	DL79	
SA 108-551.....	16 37 47.79	-00 33 05.1	Tycho	2000.000	5.50	1.20	5.10	1.20	TYC2	A0	DL79	
Wolf 629	16 55 25.66	-08 19 13.1	HIP 82809	2000.000	-813.43	4.43	-895.17	2.46	HIP	M3.5 V	HK94	m, 26
BD +18°3407.....	17 35 19.89	+ 18 53 00.8	HIP 86063	2000.000	71.00	1.10	-314.00	1.10	TYC2	G5	SIMBAD	
BD +2°3375.....	17 39 45.59	+ 02 24 59.6	HIP 86443	2000.000	-367.00	1.30	73.80	1.20	TYC2	sdG0	C83	
SA 109-71	17 44 06.78	-00 24 57.8	Tycho	2000.000	-0.60	1.50	0.00	1.50	TYC2	A0	DL79	
SA 109-381.....	17 44 12.26	-00 20 32.7	Tycho	2000.000	-2.40	1.60	4.00	1.50	TYC2	F2:	DL79	
SA 109-231.....	17 45 19.95	-00 25 51.6	Tycho	2000.000	2.40	0.80	-14.30	0.90	TYC2	K2 II	DL79	
SA 109-537.....	17 45 42.45	-00 21 35.4	Tycho	2000.000	1.00	1.20	-1.90	1.20	TYC2	F1	DL79	
Hilt 733	18 17 23.32	-11 44 57.5	Tycho	2000.000	-0.70	2.20	-4.30	2.20	TYC2	B1: II:	H56	
Ross 711	18 35 19.17	+ 28 41 55.3	HIP 91129	2000.000	-16.30	1.90	-276.60	1.90	TYC2	sdA7	G54	m, 27
SA 110-232.....	18 40 52.33	+ 00 01 54.8	Tycho	2000.000	-11.40	2.50	-25.60	2.60	TYC2	...		
SA 110-340.....	18 41 28.44	+ 00 15 23.0	Tycho	2000.000	2.70	1.10	-6.90	1.10	TYC2	A5 II	MSS99	28
SA 110-499.....	18 43 07.66	+ 00 28 01.4	Tycho	2000.000	3.90	1.70	-0.30	1.70	TYC2	B9	DL79	
SA 110-503.....	18 43 11.69	+ 00 29 42.9	Tycho	2000.000	3.10	1.60	-6.80	1.60	TYC2	A0	DL79	
GJ 745A.....	19 07 05.57	+ 20 53 16.9	HIP 93873	2000.000	-473.70	1.60	-350.30	1.60	TYC2	M1.5	MSU	
GJ 745B.....	19 07 13.19	+ 20 52 37.2	HIP 93899	2000.000	-479.30	1.70	-333.40	1.60	TYC2	M2	MSU	
BD +35°3659.....	19 31 09.22	+ 36 09 10.1	HIP 95996	2000.000	-9.20	1.90	-563.70	1.90	TYC2	sdF7	Ro55	m
SA 111-775.....	19 37 16.36	+ 00 12 05.5	Tycho	2000.000	-2.20	1.60	-6.70	1.70	TYC2	...		m
SA 111-1925.....	19 37 28.62	+ 00 25 03.1	GSC 00478-01393	1983.680	A0	DL79		
Wolf 1346	20 34 21.89	+ 25 03 49.7	HIP 101516	2000.000	-402.60	1.70	-563.30	1.70	TYC2	DA2.5	HBS98	m, p, w, 29
SA 112-223.....	20 42 14.58	+ 00 08 59.7	Tycho	2000.000	6.30	1.50	-10.70	1.50	TYC2	F5	DL79	
SA 112-250.....	20 42 26.38	+ 00 07 42.4	Tycho	2000.000	1.00	1.60	-9.50	1.70	TYC2	F8	DL79	
SA 112-805.....	20 42 46.74	+ 00 16 08.4	GSC 00511-01428	1983.683	A1	DL79		
SA 112-822.....	20 42 54.90	+ 00 15 01.9	Tycho	2000.000	-4.50	1.70	-13.20	1.80	TYC2	G8 III	DL79	
BD +62°1916.....	21 15 05.74	+ 62 50 27.9	HIP 104913	2000.000	122.40	2.00	259.50	2.00	TYC2	G5	DM91	m
SA 113-339.....	21 40 55.64	+ 00 27 58.2	GSC 00543-01300	1983.683	F8	DL79		
SA 113-466.....	21 41 27.39	+ 00 40 15.6	Tycho	2000.000	19.60	1.20	7.90	1.20	TYC2	F5	DL79	
SA 113-259.....	21 41 44.84	+ 00 17 39.9	Tycho	1991.600	K0 III	DL79		
SA 113-260.....	21 41 48.03	+ 00 23 53.3	GSC 00543-01222	1983.683		
SA 113-475.....	21 41 51.30	+ 00 39 20.8	Tycho	2000.000	16.50	1.40	-15.20	1.40	TYC2	G9 III	DL79	
BD +28°4211.....	21 51 11.02	+ 28 51 50.4	HIP 107864	2000.000	-36.90	2.00	-56.60	2.00	TYC2	Op	JM53	s, w, 30

TABLE 9—Continued

Star Name (1)	α (J2000) (2)	δ (J2000) (3)	Other ID (4)	Epoch (yr) (5)	$\mu(\alpha \cos \delta)$ (mas yr $^{-1}$) (6)	$\sigma(\mu(\alpha \cos \delta))$ (mas yr $^{-1}$) (7)	$\mu(\delta)$ (mas yr $^{-1}$) (8)	$\sigma(\mu(\delta))$ (mas yr $^{-1}$) (9)	PM Ref. (10)	Spectral Type (11)	Spectrum Ref. (12)	Notes (13)
G93-48.....	21 52 25.37	+ 02 23 19.6	HIP 107968	2000.000	14.10	2.10	-300.40	2.10	TYC2	DA3	GE87	s, 31
BD +25°4655.....	21 59 41.96	+ 26 25 57.3	HIP 108578	2000.000	-37.70	1.30	-44.40	1.20	TYC2	sdO0	GS74	32
Hilt 1089.....	22 09 20.87	+ 57 51 28.4	Tycho	2000.000	-2.30	2.90	-1.70	2.90	TYC2	B0.5n (V)	H56	
BD +17°4708.....	22 11 31.37	+ 18 05 34.1	HIP 109558	2000.000	507.20	1.30	57.60	1.3	TYC2	sdF8	SIMBAD	m
BD -11°5781.....	22 13 10.68	-11 10 38.4	HIP 109695	2000.000	288.60	1.80	-91.90	1.80	TYC2	K1 V	MSS99	33
SA 114-531.....	22 40 36.78	+ 00 51 55.6	GSC 00568-00830	1982.842		G5	DL79	
SA 114-654.....	22 41 26.14	+ 01 10 10.7	Tycho	2000.000	34.00	1.40	-11.80	1.40	TYC2	G0	DL79	
SA 114-656.....	22 41 35.06	+ 01 11 09.8	GSC 00568-01464	1982.842	
SA 114-548.....	22 41 36.83	+ 00 59 05.7	Tycho	2000.000	-1.60	2.80	-7.20	3.10	TYC2	K2:	DL79	
SA 114-750.....	22 41 44.70	+ 01 12 36.2	Tycho	2000.000	-11.20	1.60	-24.10	1.60	TYC2	B9	DL79	
G27-45.....	22 44 56.30	-02 21 12.8	HIP 112310	2000.000	738.30	1.80	-243.10	1.90	TYC2	K0	YTP95	m
Ross 786.....	23 09 33.34	+ 00 43 02.1	Tycho	2000.000	-258.00	39.00	-1280.00	39.00	TYC1	sdG2	YTP95	m, 34
GD 246.....	23 12 23.07	+ 10 47 04.2	GSC 01164-01078	2000.000	1414.00	34.00	-22.00	34.00	TF97	DA1	HBS98	m, w, 35
BD +38°4955.....	23 13 38.81	+ 39 25 02.6	HIP 114661	2000.000	168.60	3.10	-314.10	3.10	TYC2	sdF0	C83	m
BD +33°4737.....	23 34 36.13	+ 34 02 22.2	HIP 116351	2000.000	360.60	1.50	166.00	1.50	TYC2	K2	J66	36
PG 2336+004B.....	23 38 38.26	+ 00 42 46.4	GSC 00585-00720	1983.680	
SA 115-420.....	23 42 36.48	+ 01 05 58.8	Tycho	2000.000	-7.50	1.60	-3.80	1.60	TYC2	F5	DL79	
SA 115-516.....	23 44 15.38	+ 01 14 12.5	Tycho	2000.000	31.80	1.60	-21.30	1.60	TYC2	G8 IV	DL79	

NOTES.—(m) High proper motion star; (p) *Hubble Space Telescope* and/or IUE photometric standard; (s) *Hubble Space Telescope* and/or far-UV spectrophotometric standard; (w) white dwarf; (1) heavily reddened; (2) not listed in Villanova white dwarf catalog (McCook & Sion 1999); =EGGR 382, LTT 300, G270-8, USNO 490; (3) blue straggler in Per OB1 association; (4) =WD 0227+050, EG 19; (5) the northern star in an optical pair; (6) optical double, separation 0°95'; (7) listed as G5 III in SIMBAD; (8) =HD 259211; (9) listed as K7 (MSU), W94 notes as long-term variable; (10) W94 notes as long-term variable, dM4, =“Luyten’s star”; (11) listed as B2 III in SIMBAD; (12) listed as B9 V in SIMBAD; (13) the southern star in an optical pair; (14) listed as G0 by Kuiper in B85, =LTT 12271; (15) integrated magnitude and spectral type, separation 0°66'; (16) the southwest star in an optical double (Carney & Latham 1987); (17) =WD 1031–114, EG 70, LTT 3870; (18) =WD 1036+433; (19) =WD 1105–048, LP 672-1, EG 76, LTT 4099, GJ 1152B; (20) =LP 672-2, GJ 1152A; (21) listed as G0 III in SIMBAD; (22) listed as sdK in G97, sdK4 in P43; (23) listed as M4 in MSU, suspected variable, =GL 512A; (24) listed as G8 V in SIMBAD, =Gl 518.2B, western star of optical pair; (25) listed as A5p in Landolt 1973; (26) =GJ 643; (27) listed as A8 in SIMBAD and newer papers; (28) =HD 172652; (29) =WD 2032+248, EG 139, LTT 16005, G186-31, Gl 794, LHS 3562, LFT 1554, AC +25°68981; (30) listed as DA in Villanova white dwarf catalog (McCook & Sion 1999); =WD 2148+286; (31) =WD 2149+021, EG 150, G1 838.4; (32) low-amplitude variable, =IS Peg (ZZ Ceti type); (33) integrated magnitude and spectral type, separation 0.93'; (34) listed as sdG in G97, G2 VI in Heintz 1994; (35) =WD 2309+105, EG 233, BPM 97895; (36) listed as K0 in SIMBAD.

REFERENCES.—(B85) Bidelman 1985; (BH80) Berger & Fringant 1980; (C83) Carney 1983; (CH67) Cowley, Hiltner, & Witt 1967; (DB90) Doyle & Butler 1990; (DL79) Drilling & Landolt 1979; (DM91) Duquennoy & Mayor 1991; (E96) Elkin 1996; (ES59) Eggen & Sandage 1959; (G54) Greenstein 1954; (G78) Giclas, Burnham, & Thomas 1978; (G84) Greenstein 1984; (G97) Gizis 1997; (GE87) McCook & Sion 1987; (GS74) Greenstein & Sargent 1974; (H56) Hiltner 1956; (HBS98) Holberg, Barstow, & Sion 1998; (HD) Cannon & Pickering 1918–1924; (HD80) Harrington & Dahn 1980; (HIP) ESA 1997; (HK94) Henry, Kirkpatrick, & Simons 1994; (Ir58) Iriarte 1958; (J66) Jones 1967; (JM53) Johnson & Morgan 1953; (LD95) Little et al. 1995; (MSS88) Houk & Smith-Moore 1988; (MSS99) Houk & Swift 1999; (MSU) Reid, Hawley, & Gizis 1995; (NLTT) Luyten 1979–1980; (P42) Popper 1942; (P43) Popper 1943; (Ro55) Roman 1955; (S69) Sandage 1969; (S96) Stone 1996; (SAO) Astronomical Data Center 1991; (T90) Turnshek et al. 1990; (TF97) Thejll et al. 1997; (TYC1) ESA 1997; (TYC2) Høg et al. 2000; (W94) Weis 1994; (YTP95) van Altena, Lee, & Hoffleit 1995.

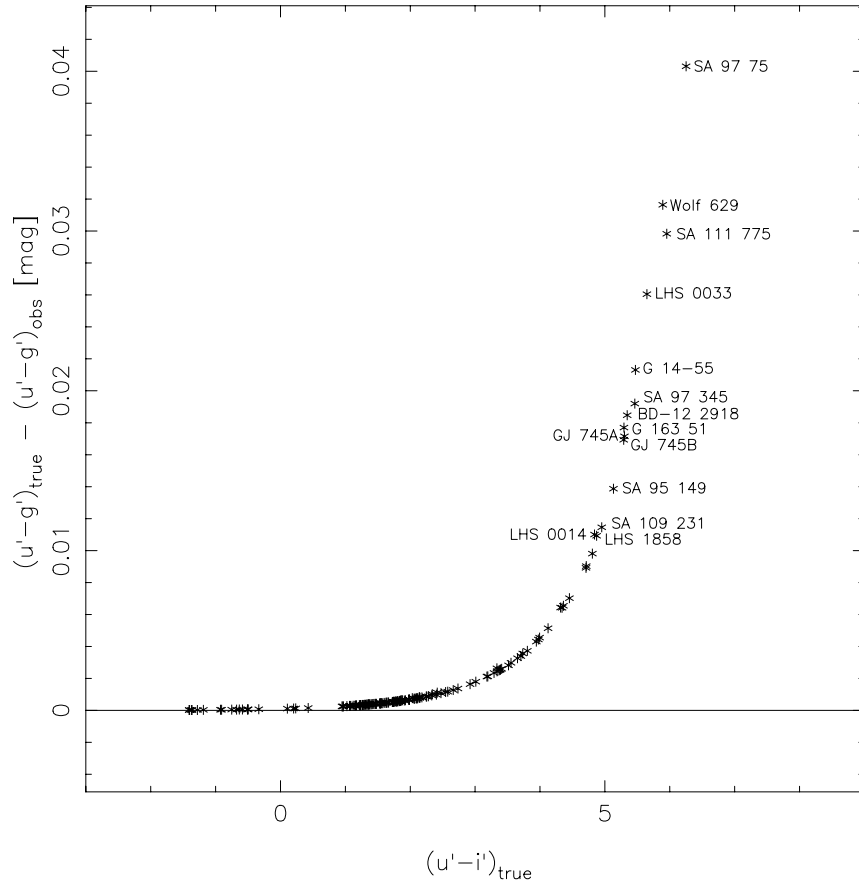


FIG. 15.—Red-leak correction $[(u' - g')_{\text{true}} - (u' - g')_{\text{obs}}]$ vs. red-leak-corrected $u' - i'$ colors for all 158 $u'g'r'i'z'$ standards. Note that for all but a handful of stars, the red-leak correction is less than 0.01 mag. Those stars with a red-leak correction greater than 0.01 mag are explicitly labeled.

and the Max-Planck-Gesellschaft. The official SDSS Web site is <http://www.sdss.org>.

The authors would like to thank the USNO Flagstaff Station for making the telescope and detector available for the observations, and Conard Dahn, Joe Hobart, Fred Harris, and Hugh Harris for their assistance during the observing sessions. We also thank David Hogg, Michael Strauss, and Gillian Knapp for their valuable reading of the manuscript and comments. J. A. S. also acknowledges the many useful discussions of the project with Conard Dahn and Hugh

Harris at USNO, Arlo Landolt at Louisiana State University, and Brian Skiff at Lowell Observatory. J. A. S. further acknowledges Lowell Observatory for its support and hospitality during the observing runs. J. A. S. and D. L. T. acknowledge Jeanne Odermann and Sahar Allam for their help in proofreading the text. Finally, we acknowledge the referee, B. Oke, for his many insightful suggestions, which have substantially improved the quality of the paper and presentation of the data. This research has made use of the SIMBAD database, operated at CDS, Strasbourg, France.

REFERENCES

- Astronomical Data Center. 1991, SAO Star Catalog J2000, in Selected Astronomical Catalogs, Vol. 1 (ADC/NSSDC CD-ROM) (Greenbelt, MD: GSFC)
- Bemporad, A. 1904, Mitt. Grossherzoglichen Sternw. Heidelberg, No. 4
- Berger, J., & Fringant, A.-M. 1980, A&A, 85, 367
- Bidelman, W. P. 1985, ApJS, 59, 197
- Cannon, A. J., & Pickering, E. C. 1918–1924, Ann. Astron. Obs. Harvard Coll., Nos. 91–100
- Carney, B. W. 1983, AJ, 88, 610
- Carney, B. W., & Latham, D. W. 1987, AJ, 93, 116
- Cowley, A. P., Hiltner, W. A., & Witt, A. N. 1967, AJ, 72, 1334
- Doyle, J. G., & Butler, C. J. 1990, A&A, 235, 335
- Drilling, J. S., & Landolt, A. U. 1979, AJ, 84, 783
- Duquennoy, A., & Mayor, M. 1991, A&A, 248, 485
- Eggen, O. J., & Sandage, A. R. 1959, MNRAS, 119, 255
- Elkin, V. G. 1996, A&A, 312, L5 (erratum 320, 681 [1997])
- ESA. 1997, The Hipparcos and Tycho Catalogues (ESA SP-1200) (Noordwijk: ESA)
- Fukugita, M., Ichikawa, T., Gunn, J. E., Doi, M., Shimasaku, K., & Schneider, D. P. 1996, AJ, 111, 1748
- Giclas, H. L., Burnham, R., Jr., & Thomas, N. G. 1978, Lowell Obs. Bull., 8, 89
- Gizis, J. E. 1997, AJ, 113, 806
- Greenstein, J. L. 1954, PASP, 66, 126
- . 1984, ApJ, 276, 602
- Greenstein, J. L., & Sargent, A. I. 1974, ApJS, 28, 157
- Gunn, J. E., et al. 1998, AJ, 116, 3040
- Harrington, R. S., & Dahn, C. C. 1980, AJ, 85, 454 (erratum 86, 1414 [1981])
- Heintz, W. D. 1994, AJ, 108, 2338
- Henry, T. J., Kirkpatrick, J. D., & Simons, D. A. 1994, AJ, 108, 1437
- Hiltner, W. A. 1956, ApJS, 2, 389
- Høg, E., et al. 2000, A&A, 355, L27
- Holberg, J. B., Barstow, M. A., & Sion, E. M. 1998, ApJS, 119, 207
- Houk, N., & Smith-Moore, M. 1988, Michigan Catalogue of Two-dimensional Spectral Types for the HD Stars, Vol. 4 (Ann Arbor: Dept. Astron., Univ. Michigan)
- Houk, N., & Swift, C. 1999, Michigan Catalogue of Two-dimensional Spectral Types for the HD Stars, Vol. 5 (Ann Arbor: Dept. Astron., Univ. Michigan)
- Iriarte, B. 1958, ApJ, 127, 507
- Johnson, H. L., & Morgan, W. W. 1953, ApJ, 117, 313
- Jones, D. H. P. 1967, R. Obs. Bull., No. 126
- Jorgensen, A. M., et al. 2002, in preparation

- Kent, S. M. 1985, PASP, 97, 165
 Landolt, A. U. 1973, AJ, 78, 959
 _____. 1983, AJ, 88, 439
 _____. 1992, AJ, 104, 372
 Lasker, B. M., Russel, J. N., & Jenkner, H. 1999, The *HST* Guide Star Catalog (version GSC-ACT; Bowdoinham, ME: Project Pluto)
 Little, J. E., Dufton, P. L., Keenan, F. P., Hambley, N. C., Conlon, E. S., Brown, P. J. F., & Miller, L. 1995, ApJ, 447, 783
 Luyten, W. J. 1979-1980, NLTT Catalogue, Vols. 1-4 (Minneapolis: Univ. Minnesota)
 McCook, G. P., & Sion, E. M. 1987, ApJS, 65, 603
 _____. 1999, ApJS, 121, 1
 Mermilliod, J.-C., Mermilliod, M., & Hauck, B. 1997, A&AS, 124, 349
 Oke, J. B. 1990, AJ, 99, 1621
 Oke, J. B., & Gunn, J. E. 1983, ApJ, 266, 713
 Popper, D. M. 1942, ApJ, 95, 307
 _____. 1943, ApJ, 98, 209
 Reid, I. N., Hawley, S. L., & Gizis, J. E. 1995, AJ, 110, 1838
 Roman, N. G. 1955, ApJS, 2, 195
 Sandage, A. 1964, ApJ, 139, 442
 Sandage, A. 1969, ApJ, 158, 1115
 Sergey, G., Berman, E., Huang, C.-H., Kent, S., Newberg, H., Nicinski, T., Petravick, D., & Stoughton, C. 1996, in ASP Conf. Ser. 101, Astronomical Data Analysis Software and Systems V, ed. G. H. Jacoby & J. Barnes (San Francisco: ASP), 248
 Smith, J. A., et al. 2002, in preparation
 Stone, R. P. S. 1977, ApJ, 218, 767
 _____. 1996, ApJS, 107, 423
 Stoughton, C. 1995, BAAS, 187, No. 91.01
 Stoughton, C., et al. 2002, AJ, 123, 485
 Thejli, P., Flynn, C., Williamson, R., & Saffer, R. 1997, A&A, 317, 689
 Thuan, T. X., & Gunn, J. E. 1976, PASP, 88, 543
 Tucker, D. L., et al. 2002, in preparation
 Turnshek, D. A., Bohlin, R. C., Williamson, R. L., II, Lupie, O. L., Koornneef, J., & Morgan, D. H. 1990, AJ, 99, 1243
 van Altena, W., Lee, J. T., & Hoffleit, D. 1995, The General Catalogue of Trigonometric Stellar Parallaxes (4th rev. ed.; New Haven: Yale Univ. Obs.)
 Veeder, G. J. 1974, AJ, 79, 1056
 Weis, E. W. 1994, AJ, 107, 1135
 York, D. G., et al. 2000, AJ, 120, 1579